

Synthesis and Biological Evaluation of Novel Triazine Derivatives as Positive Allosteric Modulators of $\alpha 7$ Nicotinic Acetylcholine Receptors

Xintong Wang, Haoran Xiao, Jing Wang, Zongze Huang, Geng Peng, Wenjun Xie, Xiling Bian, Huijie Liu, Cheng Shi, Taoyi Yang, Xin Li, Jian Gao, Ying Meng, Qianchen Jiang, Wei Chen, Fang Hu, Ningning Wei, Xiaowei Wang, Liangren Zhang, KeWei Wang,* and Qi Sun*



Cite This: *J. Med. Chem.* 2021, 64, 12379–12396



Read Online

ACCESS |



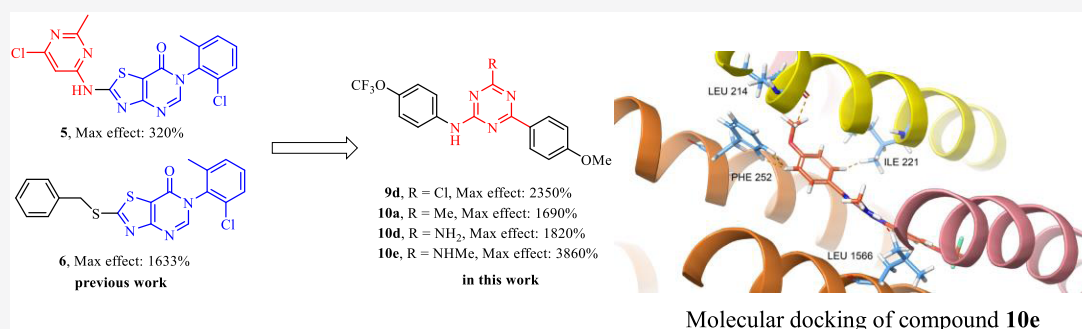
Metrics & More



Article Recommendations



Supporting Information



ABSTRACT: Enhancing neuronal $\alpha 7$ nicotinic acetylcholine receptor ($\alpha 7$ nAChR) function can alleviate cognitive deficits. Here, we report the design, synthesis, and evaluation of *N*-(4-(trifluoromethoxy)phenyl)-1,3,5-triazin-2-amine derivatives **8–10** as a series of novel $\alpha 7$ nAChR positive allosteric modulators (PAMs). The representative compound **10e** functions as a type I PAM with an EC_{50} of 3.0 μ M and approximately 38-fold enhancement of $\alpha 7$ current in the presence of agonist acetylcholine (100 μ M). It specifically enhances $\alpha 7$ current with high selectivity. Compound **10e** shows good pharmacokinetic property in mice. Intraperitoneal injection of **10e** (3 mg/kg) exhibits sufficient blood–brain barrier penetration in mice. Furthermore, **10e** can also rescue the auditory gating deficit in mice with schizophrenia-like behavior. Molecular docking of **10e** with homopentameric $\alpha 7$ nAChR reveals a new mode of action. These results support the potential of **10e** for treatment for schizophrenia and Alzheimer's disease.

INTRODUCTION

As ligand-gated ion channels, nicotinic acetylcholine receptors (nAChRs) are activated by the neurotransmitter acetylcholine (ACh) or natural alkaloid nicotine for neuronal signaling.¹ The pentameric $\alpha 7$ nAChR is a major neuronal subtype of the nAChR family in the central nervous system (CNS) with predominant expression in the brain regions, such as hippocampus and cortex.² The $\alpha 7$ nAChR is critical for cognition, sensory processing, and memory, and dysfunctional $\alpha 7$ is related to neuropsychiatric disorders, such as Alzheimer's disease and schizophrenia.³ In addition, auditory gating deficits are ubiquitous in patients with schizophrenia.⁴ Therefore, enhancing $\alpha 7$ nAChR appears to be a therapeutic strategy for potential therapy of neuropsychiatric disorders.

The positive allosteric modulators (PAMs) of $\alpha 7$ nAChR have been proposed for potential therapy of cognitive deficits.^{5,6} Unlike $\alpha 7$ agonists exhibiting paucity of effects and lack of sufficient selectivity, $\alpha 7$ PAMs can modulate the channel function by binding to their allosteric sites and are only efficacious in the presence of endogenous acetylcholine or

exogenous agonists, thus giving rise to better selectivity profile, structural diversity, and greater efficacy with extra neuroprotection.^{5a} The $\alpha 7$ PAMs can be classified into type I and type II PAMs based on their effects on macroscopic current gating kinetics.^{5b} The first selective type II PAM **1a** (PNU-120596, Figure 1) has been shown to improve the auditory gating deficit caused by amphetamine.^{6a} The effects of **1a** on lipopolysaccharide (LPS)-induced anxiety, cognitive deficit, and depression-like behaviors in mice were also determined by Rahman research group in 2019.^{6b} Among other type II PAMs of benzenesulfonamide compounds **1b** (LL-00066471),⁷ **1c** (TQS),⁸ and **1d**, 4-(thiophen-3-yl)-benzenesulfonamide **1d**

Received: June 12, 2021

Published: August 10, 2021



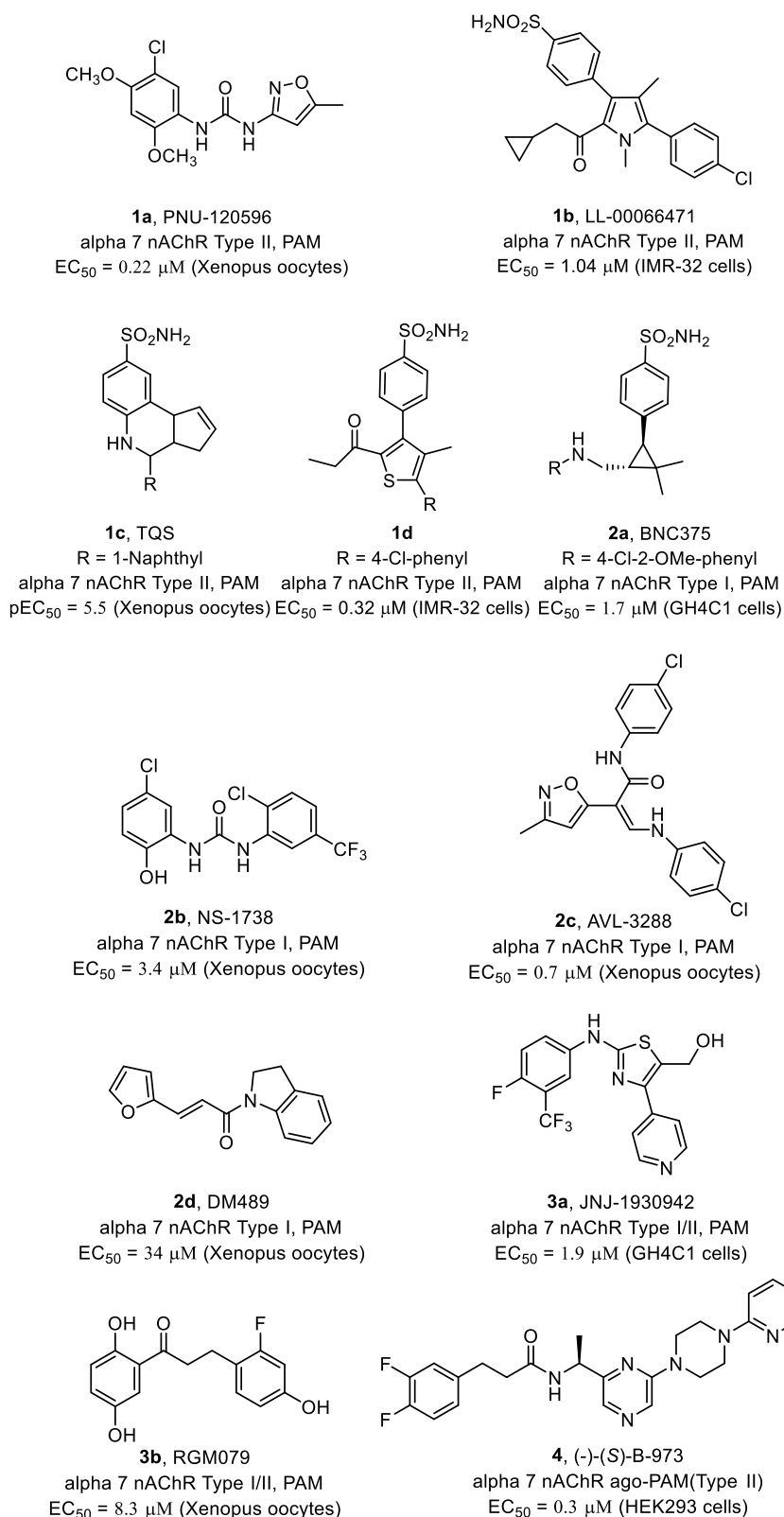


Figure 1. Representative nAChR PAMs.

showed the best allosteric effect on $\alpha 7$ nAChR (Figure 1). Compound **1d** with *in vitro* potency (EC₅₀ = 0.32 μM, IMR-32 cells) showed a reversal of cognitive deficits in episodic/working memory in both time-delay and scopolamine-induced amnesia paradigms in the novel object and social recognition tasks and safety in phase 1 clinical trials.⁹

Type II PAMs, which largely retard current desensitization kinetics, may render Ca²⁺-induced neurotoxicity. In contrast, type I PAMs exhibit rapid current desensitization kinetics.¹⁰ These representative compounds are **2a** (BNC375, EC₅₀ = 1.7 μM),¹¹ **2b** (NS1738, EC₅₀ = 3.4 μM),¹² **2c** (AVL-3288, EC₅₀ = 0.7 μM),¹³ and amide compound **2d** (DM489, EC₅₀ = 34

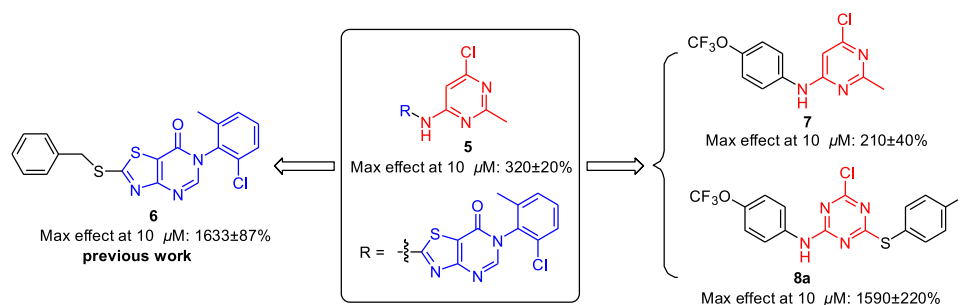
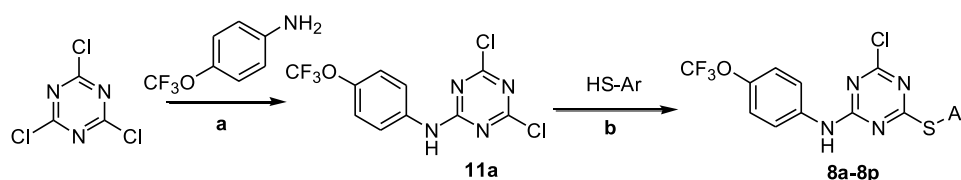


Figure 2. Hit compound **8a** of 1,3,5-triazin-2-amines.

Scheme 1



^aReagents and conditions: (a) K_2CO_3 , THF, 0 °C, then r.t., 57%; (b) Et_3N /THF 0 °C, then r.t., 22–97%.

μM)¹⁴ shown in Figure 1. **2c**, which was the best type I $\alpha 7$ nAChR allosteric modulator, could reverse schizophrenia-like deficits induced by ketamine in rats. In a clinical trial of phase 1b in 24 subjects with schizophrenia or schizoaffective disorder, AVL-3288 shows a lack of clinical effect.^{13d} Novel **3a** (JNJ-1930942, mixed type I/II PAM, Figure 1),¹⁵ **3b** (RGM079, mixed type I/II PAM, Figure 1),¹⁶ and piperazine **4** (B-973, Ago-PAM, Figure 1)¹⁷ were successively reported for the purpose of improved pharmacological activities in recent years. In addition, compound **1d** is carried phase 1 clinical study (ref 9). Therefore, selective $\alpha 7$ nicotinic receptor positive allosteric modulator may hold a promise for potential therapy of schizophrenia and related cognitive deficits.¹⁸

Our research group has recently been engaged in the identification of selective $\alpha 7$ nicotinic receptor positive allosteric modulators. Based on the structural modifications on the initial hit compound **5**, we identified a novel thiazolo[4,5-*d*]pyrimidin-7(6*H*)-one, **6** (Figure 2) as a type I PAM that enhances $\alpha 7$ current with an EC_{50} of 1.26 μM . The maximum activation of current in the presence of acetylcholine (100 μM) exceeds 1633%.¹⁹ Compound **6** is highly specific for $\alpha 7$ nAChR over other subtypes of nAChRs as well as 5-HT_{3A}, N-methyl-D-aspartic acid (NMDA), and GABA_A receptors. Compound **6** also exhibits a dose-dependent (0.1–1 mg/kg, intraperitoneally (ip)) reversal of prepulse inhibition (PPI) deficit induced by MK-801 in a mouse model of schizophrenia.

To further investigate the effect of the 4-amino-pyrimidine motif (red part of the hit compound **5**, Figure 2), we attempted to synthesize 4-amino-pyrimidine derivative **7**. However, compound **7** (the maximum $\alpha 7$ current activation is approximately 210%) showed no obvious enhancement of $\alpha 7$ currents expressed in *Xenopus* oocytes in two-electrode voltage clamp (TEVC) recordings. Literature results indicate that 1,3,5-triazine is a privileged motif and is commonly used in drug candidates with various activities, including potential anticancer activities,²⁰ antiviral activities,²¹ analgesic and anti-inflammatory activity,²² and antiparasitic activities,²³ for treating neurological disorders²⁴ and ion-channel-related diseases.²⁵ We, therefore, introduced 1,3,5-triazin-2-amine instead of 4-amino-pyrimidine in compound **7**. Appropriate

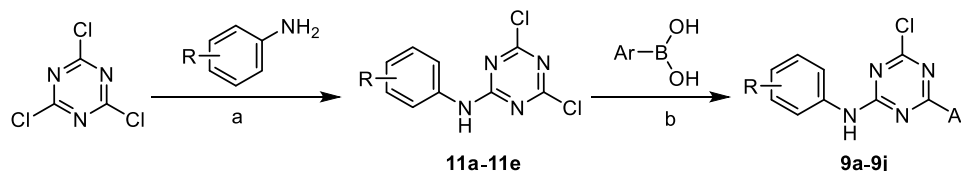
modifications were performed to provide compound **8a** that showed a maximum $\alpha 7$ current activation of 1590% in the presence of 100 μM ACh (Figure 2), comparable to that of our previously reported compound **6** (1633% of current increase).¹⁹ These findings indicated that 1,3,5-triazin-2-amine could be a key pharmacophore. To the best of our knowledge, 1,3,5-triazin-2-amine derivatives have not been explored as $\alpha 7$ nAChR PAM for therapeutic applications. In this study, we report the synthesis and biological evaluation of substituted 1,3,5-triazin-2-amine derivatives **8–10** as positive allosteric modulators of $\alpha 7$ nAChRs.

Based on compound **8a**, we designed and synthesized compounds **8b–p** to explore the influence of substituents on the –SAr group. Compounds **9a–j** were further designed to avoid possible oxidation of the –S– group during *in vivo* metabolism and reduce the cLog *P* values. Based on the lead compound **9d**, different groups were introduced for substituting chloride on 1,3,5-triazine to improve the physicochemical property and generate a series of new compounds **10a–m**. Here, we report a representative compound **10e** that selectively enhances $\alpha 7$ nAChR function without altering $\alpha 7$ nAChR current desensitization kinetics. Compound **10e** shows an improved oral bioavailability and sufficient blood–brain barrier (BBB) penetration than other compounds **8b–p** and **9a–j**. *In vivo* evaluation of acoustic startle response in PPI reveals that allosteric activation of $\alpha 7$ by compound **10e** is capable of rescuing the auditory gating deficit in mice with schizophrenia-like behavior.

RESULTS AND DISCUSSION

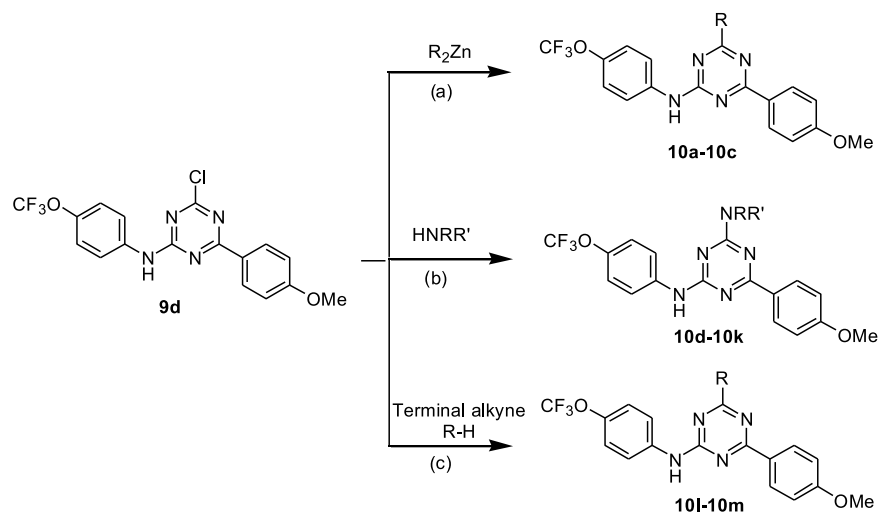
The synthesis route of 1,3,5-triazin-2-amine derivative **8** is outlined in Scheme 1. The reaction of 4-trifluoromethylphenylamine with 2,4,6-trichloro-[1,3,5]triazine produced the intermediate *N*-4-trifluoromethyl-phenyl 1,3,5-triazin-2-amine **11a** that was further treated with ArSH in the presence of potassium carbonate in tetrahydrofuran (THF) at 0 °C, then at room temperature (r.t.) overnight to produce target compounds **8a–p**. The yields of products **9a–j** produced by palladium-catalyzed Suzuki coupling reactions of **11a–e** with various aryl boronic acids were good to excellent (Scheme 2).

Scheme 2



^aReagents and conditions: (a) K_2CO_3 , THF, 0 °C, then r.t., 20–57%; (b) $Pd(Ph_3P)_4$, K_2CO_3 , THF, argon, 80 °C, 22–64%.

Scheme 3



^aReagents and conditions: (a) $Pd(PPh_3)_2Cl_2$, 1,4-dioxane, 6–9 h, 100 °C, 53–65%; (b) K_2CO_3 , THF, 65 °C, overnight (for **10d**, NH_4Cl was used instead of $NH_3 \cdot H_2O$), 43–60%; (c) $Pd(PPh_3)_2Cl_2$, dppp, CuTC, CuI, K_2CO_3 in THF at 95 °C overnight, 41–53%. $Pd(PPh_3)_2Cl_2$ = ditriphenylphosphine palladium dichloride. $Pd(PPh_3)_4$ = tetratriphenylphosphine palladium. dppp = [1,3-bis(diphenylphosphino)propane]nickel(II) chloride. CuTC = copper(I) thiophene-2-carboxylate. CuI = copper(I) iodide.

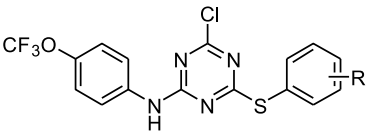
Palladium-catalyzed Negishi coupling reaction of **9d** with organic zinc reagents in the presence of $Pd(PPh_3)_2Cl_2$ in 1,4-dioxane produced the target compounds **10a–c** with good yields of 53–65% (Scheme 3, route a). The reaction of compound **9d** and 1.1 equiv of NH_4Cl in the presence of potassium carbonate in THF generated the target compound **10d** with a good yield of 60%. Compound **9d** was treated with various amine compounds in the presence of potassium carbonate in THF at 65 °C overnight to produce the target compounds **10e–k** (Scheme 3, route b). The Sonogashira coupling reaction of **9d** with propyne or *p*-methylphenylacetylene in the presence of $Pd(PPh_3)_2Cl_2$ as a catalyst in THF at 95 °C overnight resulted in the generation of products **10l** and **10m** with yields of 41 and 53%, respectively (Scheme 3, route c).

We next tested the effect of synthesized compounds on the human $\alpha 7$ nAChRs expressed in *Xenopus laevis* oocytes using the previously described two-electrode voltage clamp recording assay.²⁶ Tested compounds inactive alone at 10 μM and active in the enhancement of $\alpha 7$ current greater than 400% in the presence of ACh at 100 μM were considered as effective PAMs (Tables 1–3).

Compound **8a** (Ar = 4-F-Ph, max effect of 1590%, EC_{50} = 4.5 μM) exhibited comparable activity to compound **6** (max effect of 1633%, EC_{50} = 1.26 μM) as reported by our group in 2019.¹⁹ To further explore the SAR within the aromatic group and identify a lead compound, we examined the effects of various substituents (**8a–p**) on the phenyl group in Ar as shown in Table 1. The substitutions of 4-fluoro-phenyl on the

Ar group in **8a** with 3-fluoro-phenyl (**8b**, max effect of 970%, EC_{50} = 1.9 μM) and 2-fluoro-phenyl (**8c**, max effect of 670%, EC_{50} = 4.3 μM) resulted in a slight reduction of positive allosteric effect. Compound **8d** with 3,4-di-F-phenyl (max effect of 890%, EC_{50} = 3.3 μM) did not show the cumulative effect of difluoride atoms on PAM activity. In the following modifications, we focused on the para position of the phenyl group. Electron-withdrawing groups, such as 4-Cl (**8e**, max effect of 940%, EC_{50} = 1.7 μM), 4-Br (**8f**, max effect of 1810%, EC_{50} = 7.7 μM), and 4- CF_3 (**8g**, max effect of 680%, EC_{50} = 1.3 μM) showed good activities. In contrast, electron-donating groups 4-methyl (**8h**), 4-methoxyl (**8i**), and 4-SMe (**8j**) showed approximately 4- to 14-fold decrease in activities compared to **8a**. Substitution of 4-F with 4-hydroxyl in **8k** (max effect of 300%) also resulted in a pronounced decrease of activities. Compound **8l** (4-NHAc, max effect of 2010%, EC_{50} = 2.6 μM) had the maximum effect and moderate improvement of EC_{50} value in this series. Based on these results, it appeared that further modifying the 4-NHCOCH₃ of compound **8l** might produce more effective $\alpha 7$ PAMs. However, changing CH_3 (**8l**) with CF_3 (**8m**), Et (**8n**), Pr (**8o**) or *t*-Bu (**8p**) resulted in a decrease or loss of activity. These results suggest that a polar interaction may be formed during the interaction with the ACh ligand at the positive allosteric modulation site of the channel.

The lipophilicity of most of the active compounds in Table 1 falls outside the desired range ($1.2 < cLog P < 5.8$ (median value of 3.3) for 90% CNS drug candidates²⁷). In the evaluation of *in vitro* stability of rat liver microsomes,

Table 1. *In Vitro* Activity of Compounds 8a–p in the Enhancement of Human $\alpha 7$ nAChR Currents^a


compd	R	cLog P ^b	PSA ^b	EC ₅₀ (μM)	max effect (% at 10 μM)
8a	4-F	6.20	59.94	4.5 ± 0.5	1590 ± 220
8b	3-F	6.17	59.94	1.9 ± 0.6	970 ± 90
8c	2-F	6.15	59.94	4.3 ± 1.6	670 ± 60
8d	3,4-diF	6.29	59.94	3.3 ± 0.2	890 ± 80
8e	4-Cl	6.71	59.94	1.7 ± 0.3	940 ± 150
8f	4-Br	6.84	59.94	7.7 ± 1.6	1810 ± 110
8g	4-CF ₃	6.93	59.94	1.3 ± 0.3	680 ± 220
8h	4-Me	6.48	59.94	ND ^c	380 ± 50
8i	4-OMe	6.09	59.94	ND ^c	190 ± 20
8j	4-SMe	6.47	59.94	ND ^c	120 ± 20
8k	4-OH	5.55	59.94	ND ^c	300 ± 10
8l	4-NHAc	5.25	89.03	2.6 ± 0.5	2010 ± 210
8m	4-NHCOCF ₃	6.14	89.03	5.6 ± 1.6	950 ± 80
8n	4-NHCOEt	6.09	89.03	6.7 ± 3.8	1190 ± 90
8o	4-NHCOPr	6.65	89.03	2.6 ± 1.8	410 ± 50
8p	4-NHCO ^t Bu	6.92	89.06	ND ^c	190 ± 30

^aData were from two to five individual oocytes expressing $\alpha 7$ current. The EC₅₀ was obtained from compound concentrations that gave the half of maximum activation effect (max effect). ^bCalculated from ChemBioDraw Ultra 14.0. ^cND = not determined.

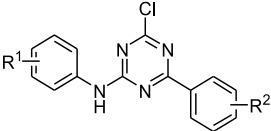
compounds 8a (max effect of 1590%, EC₅₀ = 4.5 μM), 8e (max effect of 940%, EC₅₀ = 1.7 μM), and 8l (max effect of 2010%, EC₅₀ = 2.6 μM) showed less favorable *T*_{1/2} values (8a, 27.8 min; 8e, 33.0 min; 8l, 26.6 min). These three compounds were rapidly cleared (~21–26 μL/(min·mg protein)) in rat liver microsomes (Table S1 in the Supporting Information (SI)). We envisioned that –S– could be a metabolic site for *in vitro* instability and their high lipophilicity.

To improve pharmacokinetics/pharmacodynamics (PK/PD) and identify the lead compound, compounds 9a–j were designed. These compounds were synthesized *via* the Heck coupling reaction without the –S– functional group.

Compounds 9a (R¹ = 4-OCF₃, R² = 4-NHAc), 9b (R¹ = 4-OCF₃, R² = 4-F), and 9c (R¹ = 4-OCF₃, R² = 4-Cl) showed an obvious decrease of activity comparable to 8l, 8a and 8e, respectively. In contrast, when the R² group of 4-NHAc was changed to 4-OCH₃, compound 9d (R¹ = 4-OCF₃, R² = OCH₃, max effect of 2350%, EC₅₀ = 7.9 μM, Table 2) showed a much-improved activity for positive allosteric modulation. In addition, compound 9d showed a 2-fold increase in *T*_{1/2} value at 52.5 min with a stable profile in nicotinamide adenine dinucleotide phosphate (NADPH) (Table S1 in the SI). Changing 4-OCH₃ with 3-OCH₃ or 2-OCH₃ resulted in derivatives 9e (max effect of 890%, Table 2) and 9f (max effect of 160%, Table 2) with obviously decreased activities. Therefore, in the following steps, the 4-OCH₃ group of R² was fixed and modification of R¹ was carried subsequently. A minor change of 4-OCF₃ (9d) with 4-OCH₃ (9g, max effect of 180%), 4-CF₃ (9h, max effect of 160%), 4-Me (9i, max effect of 220%), or 3-OCF₃ (9j, max effect of 170%) showed an almost complete loss of activities (Table 2). Thus, *N*-(4-(trifluoromethoxy)-phenyl)-1,3,5-triazin-2-amine appeared to be a key pharmacophore for the positive allosteric modulators of $\alpha 7$ nAChR. This conclusion was also supported by the following molecular docking results.

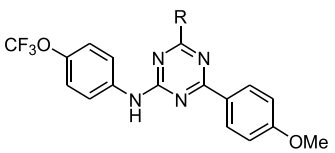
Compound 9d (max effect of 2350%, Table 2) showed an improved activity than compound 6 (max effect of 1633%), and also showed improved stability rat liver microsomes in *in vitro* (*T*_{1/2} value, 52 min, Table S1 in the SI), compared with compounds 8a, 8e, and 8l (*T*_{1/2} values about 30 min). However, compound 9d suffered from low trans-membrer potency and showed an extremely low oral bioavailability in rats (less than 1% of F value), which was not ideal for further *in vivo* pharmacological studies.

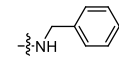
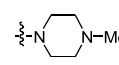
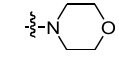
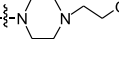
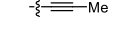
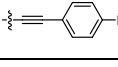
We, therefore, attempted to extend the modification of the chlorine atom for improving the polar property and its possible substitutive reaction with residue groups of the positive allosteric site of $\alpha 7$ nAChR. Compounds 10a–m listed in Table 3 were designed and synthesized. First, the methyl group was introduced to produce compound 10a (max effect of 1690%, EC₅₀ = 1.4 μM) (Table 3). Changing the methyl group with different sp³ carbon groups provided compounds 10b and 10c, respectively. Compounds 10b (max effect of 1050%, EC₅₀ = 3.4 μM, Table 3) and 10c (max effect of 500%, EC₅₀ = 6.4

Table 2. *In Vitro* Activity of Compounds 9a–j in the Enhancement of Human $\alpha 7$ nAChR Currents^{a, b}


compd	R ¹	R ²	cLog P ^(b) ^{a, b}	PSA ^(b) ^{a, b}	EC ₅₀ (μM)	max effect (% at 10 μM)
9a	4-OCF ₃	4-NHAc	4.92	89.03	4.3 ± 0.1	630 ± 120
9b	4-OCF ₃	4-F	5.86	59.94	4.4 ± 1.4	830 ± 140
9c	4-OCF ₃	4-Cl	6.38	59.94	ND	130 ± 20
9d	4-OCF ₃	4-OMe	5.76	69.17	7.9 ± 0.6	2350 ± 310
9e	4-OCF ₃	3-OMe	5.93	69.17	2.0 ± 0.1	890 ± 330
9f	4-OCF ₃	2-OMe	5.71	69.17	ND	160 ± 30
9g	4-OCH ₃	4-OMe	4.84	69.17	ND	180 ± 30
9h	4-CF ₃	4-OMe	5.68	59.94	ND	160 ± 40
9i	4-Me	4-OMe	5.24	59.94	ND	220 ± 50
9j	3-OCF ₃	4-OMe	5.73	69.17	ND	170 ± 30

^{a, b}As seen in Table 1.

Table 3. *In Vitro* Activity of Compounds 10a–m in the Enhancement of Human $\alpha 7$ nAChR Currents^a


compd	R	cLogP ^b	PSA ^b	EC ₅₀ (μM)	Max effect (% at 10 μM)
10a	-Me	4.84	69.17	1.4 ± 0.2	1690 ± 420
10b	-Et	5.42	69.17	3.4 ± 0.2	1050 ± 20
10c	-Pr	5.92	69.17	6.4 ± 0.4	500 ± 20
10d	-NH ₂	4.56	95.19	3.2 ± 0.7	1820 ± 130
10e	-NHMe	5.36	81.20	3.0 ± 0.9	3860 ± 440
10f	-NHPr	6.23	81.20	5.4 ± 0.6	450 ± 20
10g		6.75	81.20	ND	150 ± 20
10h	-N(Me)Ph	6.88	72.41	ND	270 ± 30
10i		5.61	75.65	ND	140 ± 10
10j		5.56	81.64	ND	90 ± 10
10k		4.98	95.88	11.7 ± 0.5	1960 ± 350
10l		4.62	69.17	3.8 ± 0.1	470 ± 10
10m		6.74	69.17	ND	140 ± 10

^aAs seen in Table 1. ^bAs seen in Table 1.

μM, Table 3) showed decreased activities as their cLogP values increasing. These results indicated that the modification of chlorine with a longer aliphatic chain caused poor absorption and permeation.

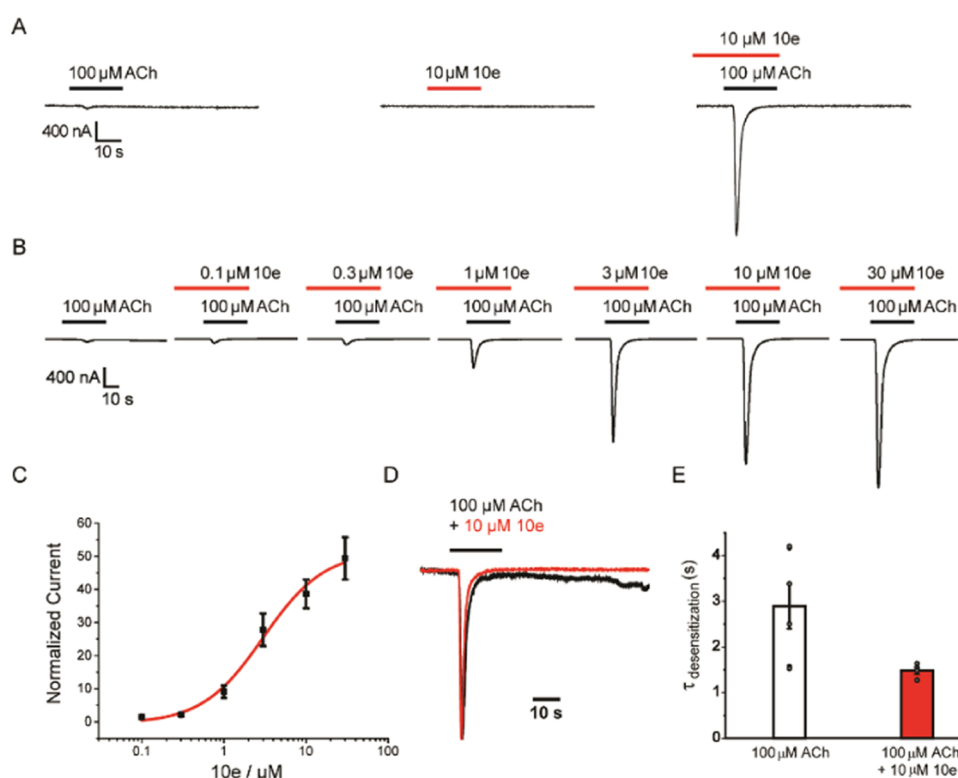
Further, the chlorine atom was substituted with different amine derivatives. Compound 10d (max effect of 1820%, EC₅₀ = 3.2 μM) exhibited good activity with an improved cLogP value of 4.56. Increasing the volume of substituents on nitrogen generated compounds 10e–h. Compound 10e (max effect of 3860%, EC₅₀ = 3.0 μM) with primary amine showed the highest positive allosteric modulation activity for $\alpha 7$ nAChRs. Substituting the -NHMe group of 10e with hydrophilic cyclic-ring groups generated compounds 10i–k. Compound 10k (max effect of 1960%, EC₅₀ = 11.7 μM) also showed good activity, which was consistent with its cLogP value of 4.98. Compound 10l (cLogP value = 4.62) was shown

to be a poor PAM of human $\alpha 7$ nAChR, with a maximum effect of 470%. Increasing the volume of alkyne to aromatic alkyne led to complete loss of activities (10m, max effect of 140%, Table 3).

Three compounds 9d (max effect of 2350%, EC₅₀ = 7.9 μM; rat liver microsomes stability assessment of $T_{1/2}$ = 53 min), 10d (max effect of 1820%, EC₅₀ = 3.2 μM; rat liver microsomes stability assessment of $T_{1/2}$ = 314 min), and 10e (max effect of 3860%, EC₅₀ = 3.0 μM; rat liver microsomes stability assessment of $T_{1/2}$ = 114 min) were analyzed to evaluate their pharmacokinetics at a dosage of 1 mg/kg (intravenously (iv)) or 10 mg/kg (orally (po)). Compound 9d showed rapid decomposition and a poor trans-membrane capacity. As shown in Figures S1 and S2, compound 9d at a dosing concentration of 1 mg/kg (iv) or 10 mg/kg (po) in rats could be seldomly detected after 3 h. The pharmacokinetic

Table 4. Noncompartmental Pharmacokinetic Parameters of **10e** in Mice Plasma after Intravenous Injection, Oral Administration, and Intraperitoneal Injection^a

parameter	administration dose			administration dose		
	10d			10e		
	1 mg/kg (iv)	3 mg/kg (po)	3 mg/kg (ip)	1 mg/kg (iv)	3 mg/kg (po)	3 mg/kg (ip)
$t_{1/2}$ (h)	0.8 ± 0.1	1.2 ± 0.3	1.3 ± 0.2	2.3 ± 0.1	1.9 ± 0.2	5.4 ± 1.3
T_{max} (h)		0.5 ± 0.0	0.4 ± 0.1		0.4 ± 0.1	0.3 ± 0.0
C_{max} (ng/mL)		60 ± 11	216 ± 34		131 ± 92	356 ± 92
AUC_{last} (ng·h/mL)	135 ± 13	112 ± 10	408 ± 79	217 ± 16	294 ± 160	651 ± 147
AUC_{inf} (ng·h/mL)	138 ± 13	125 ± 19	413 ± 77	224 ± 17	307 ± 167	669 ± 137
MRT (h)	0.7 ± 0.0	1.7 ± 0.3	1.7 ± 0.1	1.3 ± 0.1	2.5 ± 0.5	4.8 ± 1.4
V_z (L/kg)	8.8 ± 1.4			14.6 ± 1.2		
CL (mL/(min·kg))	122 ± 12			75 ± 6		
oral bioavailability (%)		30 ± 5	99 ± 18		46 ± 25	99 ± 20

^aEach measurement was repeated three times ($n = 3$).**Figure 3.** Enhancement of ACh-activated human $\alpha 7$ nAChR current by compound **10e**. (A) Current evoked by 100 μ M ACh, in the absence (left) and presence (right) of 10 μ M compound **10e**. Compound **10e** alone (middle) cannot evoke any current. (B) Representative $\alpha 7$ currents evoked by 100 μ M ACh in the absence and presence of **10e** at various concentrations. *Xenopus* oocytes were preincubated with **10e** for 2 min, followed by the co-application with 100 μ M ACh (20 s). (C) Concentration-dependent relationship of **10e** on $\alpha 7$ nAChR. *Xenopus* oocytes expressing $\alpha 7$ nAChR were activated with 100 μ M ACh in the absence and presence of increasing concentrations of **10e**. Peak currents were measured and normalized with the amplitude of currents elicited by 100 μ M ACh alone. The concentration-dependent activation of $\alpha 7$ current (100 μ M ACh) by **10e** (0.1–30 μ M) was fitted by Hill function, with an EC_{50} of $3.02 \pm 0.85 \mu$ M and an n_H of 1.17 ± 0.39 ($n = 4$). (D) Superimposition of scaled $\alpha 7$ current traces evoked with 100 μ M ACh in the absence (black) or presence (red) of 10 μ M **10e**. (E) Comparison between the desensitization kinetics ($\tau_{desensitization}$) in the absence (2.89 ± 0.49 s, $n = 6$) and presence of **10e** (1.48 ± 0.08 s, $n = 4$). Each white circle represents one single data point on each pentamer receptors.

parameters of **10d** and **10e** were determined by non-compartmental analysis using WinNonlin and are summarized in Table 4. The analysis of pharmacokinetic data showed that these two compounds were stable in plasma. The bioavailability of **10e** ($t_{1/2} = 1.9$ h, $F = 46\%$, po; $t_{1/2} = 5.4$ h, $F = 99\%$, ip; Table 4) was slightly better than that of **10d** ($t_{1/2} = 1.2$ h, $F = 30\%$, po; $t_{1/2} = 1.3$ h, $F = 99\%$, ip, Table 4). The plasma

concentration–time profiles for **10d** and **10e** under different administration routes are shown in the SI (Figures S3 and S4).

Based on the results presented above, it can be concluded that **10e** is one of the most potent PAMs for $\alpha 7$ nAChR among the target compounds. Compared with the $\alpha 7$ current amplitude evoked by 100 μ M ACh (Figure 3A, left), **10e** alone (Figure 3A, middle) was inactive for $\alpha 7$ nAChR. However, the $\alpha 7$ current amplitude had an approximately 38-

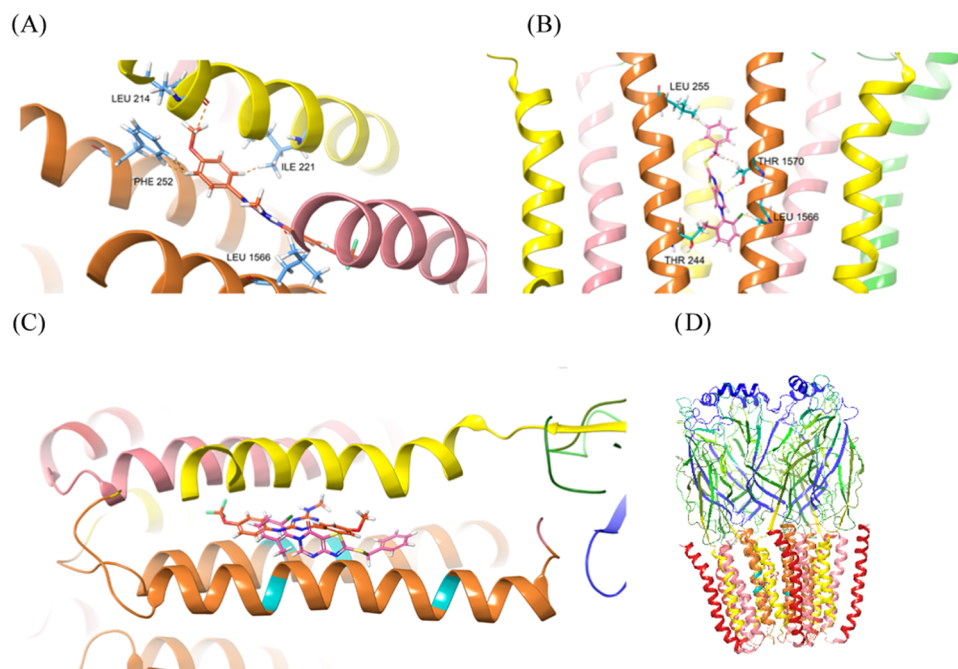


Figure 4. Docking of compounds **10e** and **6** into homopentameric $\alpha 7$ nAChR. The structure of homopentameric $\alpha 7$ was reported by Newcombe (ref 29) based on Torpedo $\alpha 7$ nAChR (PDB ID: 2BG9). (A) **10e** (brown) may interact with trans-membrane site residues L214, I221, F252, and L1566 (blue) as shown. (B) Compound **6** (pink) may interact with similar site residues L255, T1570, T244, and L1566 (green) as shown. (C) Compounds **10e** (brown) and **6** (pink) bind to the similar allosteric region of $\alpha 7$ nAChR. (D) Total image of **10e** (brown) and **6** (pink) with $\alpha 7$ nAChR.

fold increase in the presence of **10e** at 10 and 100 μM ACh (Figure 3A, right). To determine the concentration–response relationship of $\alpha 7$ current, preincubation of compound **10e** at different concentrations (0.1, 0.3, 1, 3, 10, and 30 μM) for 2 min before co-addition of 100 μM ACh resulted in $\alpha 7$ activation and rapid desensitization with an EC_{50} of $3.02 \pm 0.85 \mu\text{M}$ and E_{max} of $4941 \pm 640\%$ ($n_{\text{H}} = 1.17 \pm 0.39$, $n = 4-5$, Figure 3B–E), suggesting that **10e** is a type-I PAM of $\alpha 7$ nAChR.

Previous work by Young et al. shows that trans-membrane sites, residues S222, L247, and M253, play important roles in the allosteric modulation of $\alpha 7$ nAChR.²⁸ Some $\alpha 7$ PAMs, such as NS1738 (type I) and PNU120596 (type II) are predicted to bind to the intersubunit sites. Therefore, we selected these key amino acid residues as docking sites to perform docking. Compounds **6** and **10e** showed less favorable docking scores of -5.691 and -7.225 , respectively. We speculated that compounds **6** and **10e** may function in a new mode of action. For molecular docking, we chose the binding site reported by Newcombe et al.²⁹ The docking results suggest that our novel type I $\alpha 7$ nAChR PAM **10e** may interact with other trans-membrane sites, such as residues L214, I221, F252, and L1566, as shown in Figure 4. The residues I221, L214, and F252 with three H–H bonds as a finger interact with the CF_3O -phenyl group, which indicates that this group is essential for the allosteric effect of compound **10e**. L1566 interacts with the key skeleton 1,3,5-triazine with the H–N polar bond in the opposite direction. Compound **6** binds to a similar area, L1566 and T244 interact with the critical skeleton, while L255 and T1570 have phenylethyl groups. Our docking results show that compound **10e** (docking score: -8.147 , comparative model of the human $\alpha 7$ nAChR was generated based on Torpedo $\alpha 7$ nAChR, PDB ID: 2BG9) binds to the allosteric site of $\alpha 7$ nAChR better than

compound **6** (docking score: -7.956), which is consistent with our electrophysiological results.

Reference PAMs, such as NS1738 (type I, $\text{EC}_{50} = 3.4 \mu\text{M}$, reported max. effect of 322%) and AVL-3288 (type I, $\text{EC}_{50} = 0.7 \mu\text{M}$, reported max. effect of 900%), were performed in *Xenopus* oocytes. It seems that our compound **10e** (type I, $\text{EC}_{50} = 3.0 \mu\text{M}$, max. effect of 3860% at 10 μM) is also a potent $\alpha 7$ nAChR PAM with novel scaffold structure. The specificity of **10e** was also tested over other subtypes of nAChRs, including the $\alpha 3\beta 4$ and $\alpha 4\beta 2$ subtypes, and 5-HT_{3A} receptors that share a similar structure with nAChRs. As shown in Figures 5 and S5, **10e** and its analogues **8l** and **9d** were only able to potentiate $\alpha 7$ currents, but not $\alpha 3\beta 4$ and $\alpha 4\beta 2$ nAChRs and 5-HT_{3A} receptors. These results indicate that *N*-(4-(trifluoromethoxy)phenyl)-1,3,5-triazin-2-amine is a selective skeleton of type I $\alpha 7$ nAChR PAM.

To evaluate potential cardiac liability, we further tested the effect of **10e** on cardiac human ether-a-go-go-related gene (hERG) channel³⁰ and hNa_v1.5 channel³¹ stably expressed in Chinese hamster ovary (CHO) cells using a whole-cell patch-clamp assay. Both hERG currents and hNa_v1.5 currents were normalized to their respective controls and plotted as relative current amplitudes vs different concentrations of **10e**. As shown in Figure 6, the increased concentration of **10e** had almost no inhibitory effects on either hERG currents or hNa_v1.5 currents, suggesting that **10e** may be of less concern for cardiac toxicity.

To test the blood–brain barrier penetration, compound **10e** was administered intraperitoneally (ip) to mice at a dosage of 3 mg/kg. After administration of **10e** at 0.5, 2, and 8 h, the brain/plasma concentration ratios were 1.3, 2.3, and 2.3, respectively (Table 5 and Figure S6), demonstrating that the lead compound **10e** has an excellent brain permeability.

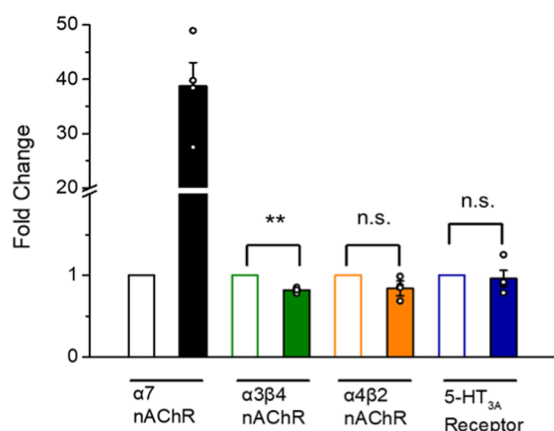


Figure 5. Selective activation of $\alpha 7$ nAChR current by compound **10e** over other subtype pentamers. The column plot shows the fold changes of $\alpha 7$ nAChR (evoked by $100 \mu\text{M}$ ACh, $n = 4$, black), $\alpha 3\beta 4$ nAChR ($100 \mu\text{M}$ ACh, $n = 4$, green), $\alpha 4\beta 2$ nAChR ($100 \mu\text{M}$ ACh, $n = 4$, orange), and 5-HT 3_A receptor ($10 \mu\text{M}$ serotonin, $n = 4$, blue) after incubation with $10 \mu\text{M}$ **10e** for 2 min. The currents co-applied with **10e** (full columns) are normalized to the currents elicited by $100 \mu\text{M}$ ACh or $10 \mu\text{M}$ serotonin (empty columns), respectively. Each white circle represents one single data point on each pentamer receptor. $**p < 0.01$, n.s., nonsignificance.

Table 5. Plasma and Brain Concentrations of **10e** in Mice after 3 mg/kg (ip) Administration^a

time point (h)	average conc. in plasma (ng/mL)	average conc. in brain (ng/g)	average brain/plasma ratio
0.5	273.0 ± 91.9	345.0 ± 94.3	1.3 ± 0.2
2	55.9 ± 16.9	128.0 ± 34.5	2.3 ± 0.1
8	14.2 ± 2.0	32.5 ± 4.1	2.3 ± 0.1

^aEach measurement was repeated three times ($n = 3$).

To evaluate the modulatory effects of **10e** on the acoustic startle response, we utilized the mouse model of schizophrenia-like PPI impairment induced by the NMDA antagonist MK-801. Intraperitoneal injection of MK-801 (0.1 mg/kg) dramatically reduced the PPI at four prepulse intensities of 8, 12, 16, and 20 dB (Figure 7A) and reduced the average PPI from 24.1 to 1.6% (Figure 7B). In contrast, the administration of different concentrations of **10e** (0.3 – 3.0 mg/kg) resulted in a dose-dependent reversal of MK-801-induced PPI impairment from 2.1 to 14.7% (Figure 7A,B). As a positive control, clozapine (1 mg/kg , ip) also reversed the PPI impairment to 16.7% (Figure 7A,B). Pretreatment with the selective $\alpha 7$ antagonist methyllycaconitine (MLA) (3 mg/kg , ip) for 30 min reduced the effect of **10e** (3 mg/kg) on reversing MK-801-induced PPI impairment to 4.7% (Figure 7B). These

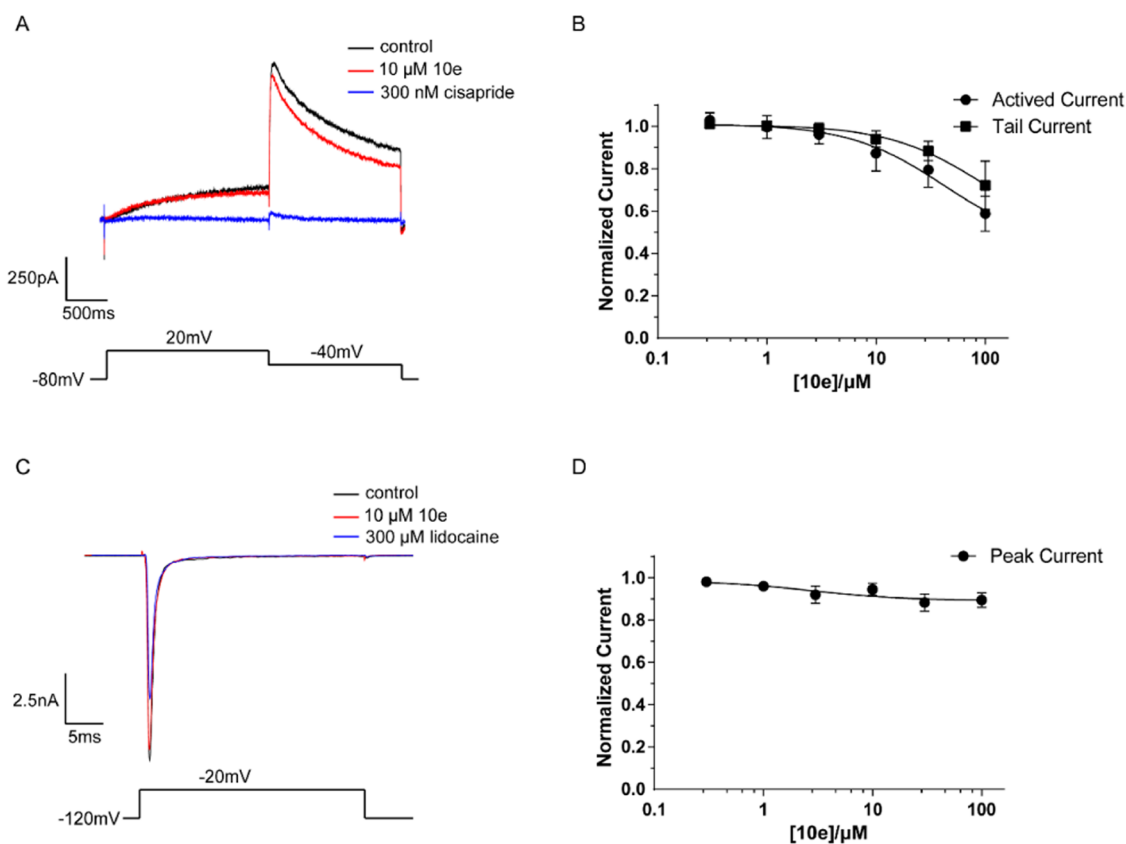


Figure 6. Lack of inhibition of cardiac hERG and hNa_v1.5 channels by **10e**. (A) Representative current traces of hERG channel activated at +20 mV and repolarized to −40 mV to evoke the characteristic hERG tail current. Black, red, and blue traces present hERG channel currents in the absence of **10e** and cisapride, in the presence of $10 \mu\text{M}$ compound **10e** or 300 nM cisapride, respectively. (B) Concentration–response relationship of compound **10e** (0.3 , 1 , 3 , 10 , and $30 \mu\text{M}$) on hERG current (black circles) and peak tail (black squares) currents. (C) Representative current traces of hNa_v1.5 channels stably expressed in human embryonic kidney (HEK) 293 cells held at −120 mV and activated at −20 mV to evoke the peak current. Black, red, and blue traces are tested in the absence of any compound, in the presence of $10 \mu\text{M}$ **10e** and 300 μM lidocaine. (D) Concentration–response relationship of compound **10e** (0.3 , 1 , 3 , 10 , $30 \mu\text{M}$) on hNa_v1.5 peak current (black circle, $n = 5$ – 7 for each point).

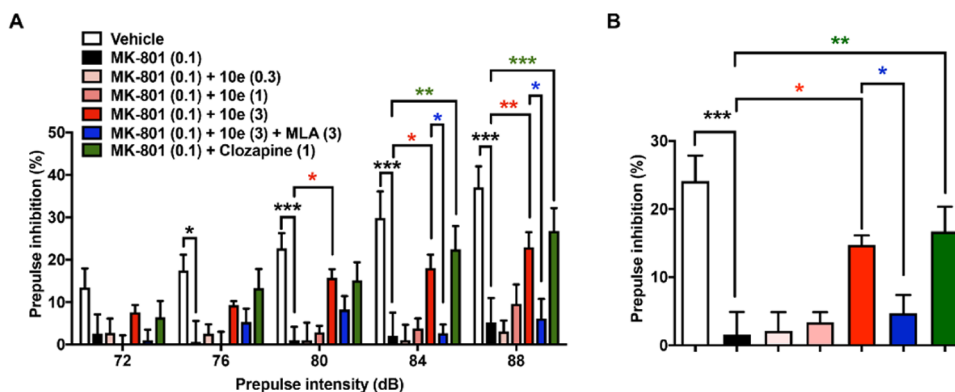


Figure 7. Reversal of acoustic startle PPI impairment by 10e. (A) Pretreatment of 10e (0.3, 1, 3 mg/kg, ip) attenuated the auditory gating deficits induced by MK-801 (0.1 mg/kg) in a dose-dependent manner, and the effect could be reversed by $\alpha 7$ nACh antagonist MLA (3 mg/kg, ip, 30 min prior). Clozapine (3 mg/kg, ip) was used as a positive control. (B) Average PPI across all of the prepulse levels (4, 8, 12, 16, and 20 dB above background noise at 68 dB) in (A). The bars are expressed as mean \pm standard error of the mean (SEM) ($n = 6$ –8 mice). * $p < 0.05$, ** $p < 0.01$, and *** $p < 0.001$, compared with the corresponding control group, two-way analysis of variance (ANOVA) or one-way ANOVA.

results indicate that type I PAM 10e can rescue the auditory gating deficit in mice through the activation of $\alpha 7$ nACh receptors.

CONCLUSIONS

In this study, we identified a novel and selective $\alpha 7$ nAChR type I PAM, compound 10e, from serial modifications of 1,3,5-triazin-2-amine derivatives using a two-electrode voltage clamp recording as a primary assay. Compound 10e showed a good pharmacokinetic profile and excellent brain tissue distribution. Peritoneal injection of compound 10e (0.3, 1, and 3 mg/kg) significantly attenuated the auditory gating deficits induced by MK-801 (0.1 mg/kg). And the effect of 10e on PPI enhancement could be reversed by $\alpha 7$ nACh antagonist MLA. Our identification of the lead compound 10e as type I PAM of $\alpha 7$ nAChR not only provides a pharmacological tool for further understanding of new aspects of $\alpha 7$ nAChR functionality, but also a potential therapy for neuropsychiatric disorders, such as schizophrenia and Alzheimer's disease.

EXPERIMENTAL SECTION

General. Commercial reagents were purchased from Ouhe, Aladdin, and J&K Scientific, and were used without further purification. ^1H and ^{13}C NMR spectra were recorded with a Bruker AVIII-400 or AVIII-600 spectrometer at ambient temperature with CDCl_3 or dimethyl sulfoxide ($\text{DMSO}-d_6$) as the solvent. Chemical shifts were referenced to the residual peaks of the solvent [CDCl_3 : $\delta = 7.26$ (^1H), 77.16 ppm (^{13}C); $\text{DMSO}-d_6$: $\delta = 2.50$ (^1H), 39.52 ppm (^{13}C)]. High-resolution mass spectra (HRMS) were recorded with a Bruker Apex IV Fourier transform ion cyclotron resonance mass spectrometer. Flash column chromatography was performed using 200–300 mesh silica gel. The purity of final compounds was verified using an Agilent 1260 instrument (Agilent Technologies, Waldbronn, Germany). The mobile phase consisted of methanol (A) and water containing 0.1% formic acid (FA) (v/v, B). The analytes were eluted using a linear gradient program: 0–20 min, 20–100% A; 20–25 min, 100% A; 26–31 min, 20% A was employed on an Agilent ZORBAX SB-C18 column ($4.6 \times 250 \text{ mm}^2$, $5 \mu\text{m}$). The flow rate was set to 1 mL/min, and the column was maintained at 30°C . The purity of final compounds was assessed using UV detection (Agilent Technologies, Waldbronn, Germany) at 254 nm; all tested compounds were $\geq 95\%$ pure. All final compounds passed the PAINS filter³² using False Positive Remover, Web-GCB13, 2010.³³ Rat liver microsome stability assessments, liquid chromatography–mass spectrometry (LC-MS) assay for pharmacokinetic analysis of 9d, 10d, and 10e, and pharmacokinetics of 10e in plasma and brain were performed in

compliance with the Ethical Review System of Laboratory Animal of Peking University. The prepulse inhibition of 10e *in vivo* was complied with the Ethical Review System of Laboratory Animal of Qingdao University.

Synthesis of Target Compounds 8–10. 4-Chloro-6-((4-fluorophenyl)thio)-N-(4-(trifluoromethoxy)phenyl)-1,3,5-triazin-2-amine (8a). Compound 11a (326 mg, 1.0 mmol) was dissolved in THF (2 mL), and a solution of 4-fluorobenzenethiol (141 mg, 1.1 mmol) and Et_3N (145 mg, 1.4 mmol) in THF (1 mL) was added in an ice bath. Then, the reaction was kept at room temperature overnight with stirring. After the completion of the reaction, the mixture was concentrated under reduced pressure. Then, water was added before quenching with ethanol. The crude material was purified by silica gel chromatography (petroleum ether (PE)/ethyl acetate (EA) = 20:1) to obtain white solid compound 8a (86% yield) with a melting point of 108.4 – 110.0°C . ^1H NMR (400 MHz, CDCl_3): δ (ppm) 7.58 (d, $J = 4.6 \text{ Hz}$, 2H), 7.32 (s, 1H), 7.18 (t, $J = 8.0 \text{ Hz}$, 2H), 7.08 (d, $J = 6.9 \text{ Hz}$, 2H), 6.97 (d, $J = 7.9 \text{ Hz}$, 2H). ^{13}C NMR (101 MHz, CDCl_3): δ (ppm) 184.9, 168.8, 164.1 (d, $J = 251.2 \text{ Hz}$), 162.4, 145.5, 138.4 (d, $J = 8.1 \text{ Hz}$), 135.2, 122.6, 121.4, 120.9, 119.1 (q, $J = 255.6 \text{ Hz}$), 116.2. HRMS (electrospray ionization (ESI)+) m/z calcd for $\text{C}_{16}\text{H}_9\text{ClF}_4\text{N}_4\text{OS}$ [$\text{M} + \text{H}$] $^+$ 417.0194, found 417.0191. HPLC purity: 99.7%, retention time = 14.9 min.

4-Chloro-6-((3-fluorophenyl)thio)-N-(4-(trifluoromethoxy)phenyl)-1,3,5-triazin-2-amine (8b). The title compound was prepared from compound 11a and 3-fluorobenzenethiol following the general procedure of 8a. White solid (65% yield). mp: 112.5 – 114.7°C . ^1H NMR (400 MHz, CDCl_3): δ (ppm) 7.56–7.34 (m, 4H), 7.31 (s, 1H), 7.12 (d, $J = 8.0 \text{ Hz}$, 2H), 6.97 (d, $J = 7.7 \text{ Hz}$, 2H). ^{13}C NMR (101 MHz, CDCl_3): δ (ppm) 184.4, 168.9, 162.7 (d, $J = 250.4 \text{ Hz}$), 162.5, 145.5, 135.1, 131.7, 130.8, 128.9, 123.1, 121.5, 119.9 (q, $J = 255.7 \text{ Hz}$), 117.2. HRMS (ESI+) m/z calcd for $\text{C}_{16}\text{H}_9\text{ClF}_4\text{N}_4\text{OS}$ [$\text{M} + \text{H}$] $^+$ 417.0194; found 417.0189. High-performance liquid chromatography (HPLC) purity: 98.2%, retention time = 16.6 min.

4-Chloro-6-((2-fluorophenyl)thio)-N-(4-(trifluoromethoxy)phenyl)-1,3,5-triazin-2-amine (8c). The title compound was prepared from compound 11a and 2-fluorobenzenethiol following the general procedure of 8a. White solid (97% yield). mp: 115.3 – 116.8°C . ^1H NMR (400 MHz, $\text{DMSO}-d_6$): δ (ppm) 10.98 (s, 1H), 7.75 (t, $J = 7.1 \text{ Hz}$, 2H), 7.52 (t, $J = 8.7 \text{ Hz}$, 1H), 7.42 (t, $J = 7.5 \text{ Hz}$, 1H), 7.31 (d, $J = 8.5 \text{ Hz}$, 2H), 7.10 (d, $J = 8.4 \text{ Hz}$, 2H). ^{13}C NMR (101 MHz, $\text{DMSO}-d_6$): δ (ppm) 182.2, 168.2, 162.7, 162.6, 144.3, 138.2, 137.2, 133.9, 126.0, 121.8 (d, $J = 255.5 \text{ Hz}$), 121.8, 119.3, 116.9, 114.4. HRMS (ESI+) m/z calcd for $\text{C}_{16}\text{H}_{10}\text{ClF}_4\text{N}_4\text{OS}$ [$\text{M} + \text{H}$] $^+$ 417.0191, found 417.0194. HPLC purity: 99.6%, retention time = 16.3 min.

4-Chloro-6-((3,4-difluorophenyl)thio)-N-(4-(trifluoromethoxy)phenyl)-1,3,5-triazin-2-amine (8d). The title compound was

prepared from compound **11a** and 3,4-difluorobenzenethiol following the general procedure of **8a**. White solid (94% yield). mp: 102.8–103.4 °C. ¹H NMR (400 MHz, CDCl₃): δ (ppm) 7.58 (s, 1H), 7.44 (d, *J* = 8.9 Hz, 1H), 7.34 (s, 1H), 7.27 (d, *J* = 8.7 Hz, 1H), 7.14 (d, *J* = 8.7 Hz, 2H), 7.02 (d, *J* = 8.4 Hz, 2H). ¹³C NMR (101 MHz, CDCl₃): δ (ppm) 184.1, 169.0, 162.5, 151.9 (dd, *J* = 253.4, 11.4 Hz), 150.3 (dd, *J* = 253.0, 13.5 Hz), 145.8, 135.0, 132.8, 125.3 (d, *J* = 17.9 Hz), 123.3, 122.2, 121.6 (q, *J* = 269.8 Hz), 119.2, 118.2 (d, *J* = 17.7 Hz). HRMS (ESI+) *m/z* calcd for C₁₆H₉ClF₅N₄OS [M + H]⁺ 435.0100, found 435.0100. HPLC purity: 99.1%, retention time = 15.1 min.

4-Chloro-6-((4-chlorophenyl)thio)-N-(4-(trifluoromethoxy)phenyl)-1,3,5-triazin-2-amine (8e). The title compound was prepared from compound **11a** and 4-chlorobenzenethiol following the general procedure of **8a**. White solid (53% yield). mp: 127.3–128.7 °C. ¹H NMR (400 MHz, CDCl₃): δ (ppm) 7.79 (d, *J* = 27.0 Hz, 1H), 7.53 (d, *J* = 7.9 Hz, 2H), 7.46 (d, *J* = 7.9 Hz, 2H), 7.07 (d, *J* = 8.8 Hz, 2H), 6.99 (d, *J* = 8.5 Hz, 2H). ¹³C NMR (101 MHz, CDCl₃): δ (ppm) 184.7, 168.7, 162.3, 145.5, 137.5, 136.8, 135.2, 129.9, 125.6, 121.4, 121.3, 120.4 (q, *J* = 257.4 Hz). HRMS (ESI+) *m/z* calcd for C₁₆H₁₀Cl₂F₃N₄OS [M + H]⁺ 432.9895, found 432.9895. HPLC purity: 98.9%, retention time = 17.3 min.

4-((4-Bromophenyl)thio)-6-chloro-N-(4-(trifluoromethoxy)phenyl)-1,3,5-triazin-2-amine (8f). The title compound was prepared from compound **11a** and 4-bromobenzenethiol following the general procedure of **8a**. White solid (22% yield). mp: 116.5–117.7 °C. ¹H NMR (400 MHz, CDCl₃): δ (ppm) 7.63 (d, *J* = 8.1 Hz, 2H), 7.47 (d, *J* = 8.1 Hz, 2H), 7.38 (s, 1H), 7.05 (d, *J* = 8.9 Hz, 2H), 7.01 (d, *J* = 8.7 Hz, 2H). ¹³C NMR (101 MHz, CDCl₃): δ (ppm) 184.6, 168.8, 162.2, 145.4, 137.7, 135.1, 132.8, 126.2, 125.0, 121.5, 121.0, 120.4 (q, *J* = 257.2 Hz). HRMS (ESI+) *m/z* calcd for C₁₆H₉BrClF₃N₄OS [M + H]⁺ 476.9394, found 476.9390. HPLC purity: 99.6%, retention time = 15.8 min.

4-Chloro-N-(4-(trifluoromethoxy)phenyl)-6-((4-(trifluoromethyl)phenyl)thio)-1,3,5-triazin-2-amine (8g). The title compound was prepared from compound **11a** and 4-(trifluoromethyl)benzenethiol following the general procedure of **8a**. White solid (31% yield). mp: 84.3–85.2 °C. ¹H NMR (400 MHz, CDCl₃): δ (ppm) 7.78 (s, 1H), 7.74 (s, 4H), 7.07 (d, *J* = 8.7 Hz, 2H), 6.93 (d, *J* = 8.4 Hz, 2H). ¹³C NMR (101 MHz, CDCl₃): δ (ppm) 184.0, 168.8, 162.4, 145.6, 136.4, 135.0, 132.4, 132.1, 131.7, 126.2, 123.7 (q, *J* = 272.2 Hz), 121.3, 120.4 (q, *J* = 257.3 Hz). HRMS (ESI+) *m/z* calcd for C₁₇H₁₀ClF₆N₄OS [M + H]⁺ 467.0158, found 467.0162. HPLC purity: 98.8%, retention time = 15.5 min.

4-Chloro-6-(*p*-tolylthio)-N-(4-(trifluoromethoxy)phenyl)-1,3,5-triazin-2-amine (8h). The title compound was prepared from compound **11a** and 4-methylbenzenethiol following the general procedure of **8a**. White solid (34% yield). mp: 160.2–161.7 °C. ¹H NMR (400 MHz, CDCl₃): δ (ppm) 7.58 (s, 1H), 7.54 (d, *J* = 6.6 Hz, 2H), 7.33 (d, *J* = 12.2 Hz, 2H), 7.13 (s, 2H), 6.93 (s, 2H), 2.54 (s, 3H). ¹³C NMR (101 MHz, CDCl₃): δ (ppm) 185.6, 168.7, 162.3, 145.1, 140.5, 136.1, 135.4, 130.4, 122.7 (q, *J* = 202.8 Hz), 121.2, 121.0, 119.2, 21.3. HRMS (ESI+) *m/z* calcd for C₁₇H₁₂ClF₃N₄OS [M + H]⁺ 413.0445, found 413.0456. HPLC purity: 99.8%, retention time = 17.4 min.

4-Chloro-6-((4-methoxyphenyl)thio)-N-(4-(trifluoromethoxy)phenyl)-1,3,5-triazin-2-amine (8i). The title compound was prepared from compound **11a** and 4-methoxybenzenethiol following the general procedure of **8a**. White solid (55% yield). mp: 138.1–140.0 °C. ¹H NMR (400 MHz, CDCl₃): δ (ppm) 7.52 (s, 1H), 7.51 (d, *J* = 8.5 Hz, 2H), 7.07 (d, *J* = 8.3 Hz, 2H), 7.01 (d, *J* = 8.0 Hz, 2H), 6.91 (d, *J* = 7.9 Hz, 2H), 3.89 (s, 3H). ¹³C NMR (101 MHz, CDCl₃): δ (ppm) 185.9, 168.6, 162.2, 161.3, 145.1, 137.8, 135.4, 121.7 (q, *J* = 255.6 Hz), 121.3, 120.9, 117.8, 115.1, 55.4. HRMS (ESI+) *m/z* calcd for C₁₇H₁₂ClF₃N₄O₂S [M + H]⁺ 429.0394, found 429.0392. HPLC purity: 99.7%, retention time = 16.6 min.

4-Chloro-6-((4-(methylthio)phenyl)thio)-N-(4-(trifluoromethoxy)phenyl)-1,3,5-triazin-2-amine (8j). The title compound was prepared from compound **11a** and 4-(methylthio)benzenethiol following the general procedure of **8a**. White solid (61% yield). mp: 142.7–144.5 °C. ¹H NMR (400 MHz, CDCl₃): δ (ppm)

7.50 (s, 1H), 7.49 (d, *J* = 7.9 Hz, 2H), 7.31 (d, *J* = 8.0 Hz, 2H), 7.06 (d, *J* = 8.8 Hz, 2H), 6.98 (d, *J* = 8.6 Hz, 2H), 2.54 (s, 3H). ¹³C NMR (101 MHz, CDCl₃): δ (ppm) 185.5, 168.7, 162.2, 145.24, 142.5, 136.5, 135.4, 126.2, 122.5, 121.5, 120.8, 120.4 (q, *J* = 257.3 Hz), 14.7. HRMS (ESI+) *m/z* calcd for C₁₇H₁₂ClF₃N₄OS₂ [M + H]⁺ 445.0166, found 445.0168. HPLC purity: 97.4%, retention time = 17.2 min.

4-((4-Chloro-6-((4-(trifluoromethoxy)phenyl)amino)-1,3,5-triazin-2-yl)thio)phenol (8k). The title compound was prepared from compound **11a** and 4-mercaptophenol following the general procedure of **8a**. White solid (53% yield). mp: 157.6–159.8 °C. ¹H NMR (400 MHz, CDCl₃): δ (ppm) 7.48 (d, *J* = 7.9 Hz, 2H), 7.34 (s, 1H), 7.10 (d, *J* = 8.4 Hz, 2H), 6.97 (t, *J* = 7.6 Hz, 4H), 5.14 (s, 1H). ¹³C NMR (101 MHz, DMSO-*d*₆): δ (ppm) 184.9, 168.0, 162.4, 160.1, 144.1, 138.3, 137.5, 121.7, 121.5, 120.5 (q, *J* = 253.1 Hz), 117.2, 115.5. HRMS (ESI+) *m/z* calcd for C₁₆H₁₀ClF₃N₄O₂S [M + H]⁺ 415.0238, found 415.0239. HPLC purity: 96.8%, retention time = 14.5 min.

N-(4-((4-Chloro-6-((4-(trifluoromethoxy)phenyl)amino)-1,3,5-triazin-2-yl)thio)phenyl)acetamide (8l). The title compound was prepared from compound **11a** and *N*-(4-mercaptophenyl)acetamide following the general procedure of **8a**. White solid (66% yield). mp: 112.1–113.0 °C. ¹H NMR (400 MHz, DMSO-*d*₆): δ (ppm) 10.84 (s, 1H), 10.33 (s, 1H), 7.79 (d, *J* = 8.6 Hz, 2H), 7.58 (d, *J* = 8.6 Hz, 2H), 7.28 (d, *J* = 9.1 Hz, 2H), 7.02 (d, *J* = 8.7 Hz, 2H), 2.12 (s, 3H). ¹³C NMR (101 MHz, DMSO-*d*₆): δ (ppm) 184.5, 169.2, 168.0, 162.4, 144.2, 141.8, 137.3, 121.7, 121.5, 120.5 (q, *J* = 256.0 Hz), 120.1, 120.0, 24.4. HRMS (ESI+) *m/z* calcd for C₁₈H₁₃ClF₃N₅O₂S [M + H]⁺ 456.0503, found 456.0502. HPLC purity: 99.1%, retention time = 15.1 min.

N-(4-((4-Chloro-6-((4-(trifluoromethoxy)phenyl)amino)-1,3,5-triazin-2-yl)thio)phenyl)-2,2,2-trifluoroacetamide (8m). The title compound was prepared from compound **11a** and 2,2,2-trifluoro-*N*-(4-mercapto-phenyl)-acetamide following the general procedure of **8a**. White solid (35% yield). mp: 170.0–170.5 °C. ¹H NMR (400 MHz, DMSO-*d*₆): δ (ppm) 11.61 (s, 1H), 10.85 (s, 1H), 7.89 (d, *J* = 8.5 Hz, 2H), 7.69 (d, *J* = 8.5 Hz, 2H), 7.24 (d, *J* = 9.0 Hz, 2H), 6.97 (d, *J* = 8.7 Hz, 2H). ¹³C NMR (101 MHz, DMSO-*d*₆): δ (ppm) 184.0, 168.1, 162.5, 155.2, 144.2, 138.9, 137.5, 137.2, 123.5, 122.0, 121.9, 121.4, 120.5 (q, *J* = 255.7 Hz), 116.1 (q, *J* = 288.6 Hz). HRMS (ESI+) *m/z* calcd for C₁₈H₁₁ClF₆N₅O₂S [M + H]⁺ 510.0215, found 510.0220. HPLC purity: 99.2%, retention time = 14.1 min.

N-(4-((4-Chloro-6-((4-(trifluoromethoxy)phenyl)amino)-1,3,5-triazin-2-yl)thio)phenyl)propionamide (8n). The title compound was prepared from compound **11a** and *N*-(4-mercapto-phenyl)-propionamide following the general procedure of **8a**. White solid (60% yield). mp: 183.7–184.4 °C. ¹H NMR (400 MHz, DMSO-*d*₆): δ (ppm) 10.83 (s, 1H), 10.25 (s, 1H), 7.80 (d, *J* = 8.1 Hz, 2H), 7.56 (d, *J* = 8.1 Hz, 2H), 7.26 (d, *J* = 8.6 Hz, 2H), 6.99 (d, *J* = 8.4 Hz, 2H), 2.39 (q, *J* = 7.3 Hz, 2H), 1.13 (t, *J* = 7.4 Hz, 3H). ¹³C NMR (101 MHz, DMSO-*d*₆): δ (ppm) 184.6, 173.0, 168.0, 162.4, 144.2, 144.1, 141.9, 137.4, 121.7, 121.5, 120.5 (q, *J* = 255.7 Hz), 120.1, 119.9, 30.1, 9.8. HRMS (ESI+) *m/z* calcd for C₁₉H₁₆ClF₃N₅O₂S [M + H]⁺ 470.0656, found 470.0659. HPLC purity: 99.0%, retention time = 13.2 min.

N-(4-((4-Chloro-6-((4-(trifluoromethoxy)phenyl)amino)-1,3,5-triazin-2-yl)thio)phenyl)butyramide (8o). The title compound was prepared from compound **11a** and *N*-(4-mercapto-phenyl)-butyramide following the general procedure of **8a**. White solid (58% yield). mp: 187.4–188.2 °C. ¹H NMR (400 MHz, DMSO-*d*₆): δ (ppm) 10.84 (s, 1H), 10.26 (s, 1H), 7.81 (d, *J* = 8.1 Hz, 2H), 7.57 (d, *J* = 8.1 Hz, 2H), 7.27 (d, *J* = 8.5 Hz, 2H), 6.99 (d, *J* = 8.4 Hz, 2H), 2.35 (d, *J* = 7.1 Hz, 2H), 1.67 (m, *J* = 14.5, 7.2 Hz, 2H), 0.96 (t, *J* = 7.3 Hz, 3H). ¹³C NMR (101 MHz, DMSO-*d*₆): δ (ppm) 184.5, 172.1, 168.0, 162.4, 144.1, 141.8, 137.4, 137.3, 121.6, 121.6, 120.5 (q, *J* = 255.8 Hz), 120.1, 119.9, 38.9, 18.9, 14.0. HRMS (ESI+) *m/z* calcd for C₂₀H₁₈ClF₃N₅O₂S [M + H]⁺ 484.0812, found 484.0816. HPLC purity: 99.7%, retention time = 13.7 min.

N-(4-((4-Chloro-6-((4-(trifluoromethoxy)phenyl)amino)-1,3,5-triazin-2-yl)thio)phenyl)pivalamide (8p). The title compound was prepared from compound **11a** and *N*-(4-mercapto-phenyl)-2,2-dimethyl-propionamide following the general procedure of **8a**.

White solid (38% yield). mp: 187.5–188.3 °C. ^1H NMR (400 MHz, DMSO- d_6): δ (ppm) 10.86 (s, 1H), 9.59 (s, 1H), 7.91 (d, J = 7.9 Hz, 2H), 7.58 (d, J = 8.0 Hz, 2H), 7.27 (d, J = 8.3 Hz, 2H), 7.00 (d, J = 8.3 Hz, 2H), 1.29 (s, 9H). ^{13}C NMR (101 MHz, DMSO- d_6): δ (ppm) 184.6, 177.4, 168.0, 162.4, 144.1, 142.0, 137.5, 137.1, 121.7, 121.6, 121.1, 120.1 (q, J = 264.2 Hz), 119.2, 27.5, 27.4. HRMS (ESI+) m/z calcd for $\text{C}_{21}\text{H}_{20}\text{ClF}_3\text{N}_3\text{O}_2\text{S}$ [$\text{M} + \text{H}$] $^+$ 498.0967, found 498.0972. HPLC purity: 98.1%, retention time = 14.1 min.

***N*-(4-(4-Chloro-6-((4-(trifluoromethoxy)phenyl)amino)-1,3,5-triazin-2-yl)phenyl)acetamide (9a).** Compound 11a (325 mg, 1.0 mmol), (4-acetamidophenyl)boronic acid (181 mg, 1.5 mmol), Pd(PPh $_3$) $_4$ (57 mg, 0.05 mmol), K $_2$ CO $_3$ (276 mg, 2.0 mmol) and THF (5 mL) was added in 35 mL sealed tubes in turn. Then, the reaction mixture was held at 70 °C overnight with stirring under the protection of argon. After the reaction was completed, EA (50 mL) was added and the mixture was filtered through celite. The mixture was concentrated under reduced pressure. The crude material was purified by silica gel chromatography (PE/EA = 15:1) to afford compound 9a as a white solid in a 20% yield. mp: 237.4–238.3 °C. ^1H NMR (400 MHz, DMSO- d_6): δ (ppm) 10.81 (s, 1H), 10.30 (s, 1H), 8.27 (d, J = 8.5 Hz, 2H), 7.89 (d, J = 8.6 Hz, 2H), 7.77 (d, J = 4.9 Hz, 2H), 7.41 (d, J = 4.9 Hz, 2H), 2.09 (s, 3H). ^{13}C NMR (101 MHz, DMSO- d_6): δ (ppm) 168.9, 164.0, 143.9, 137.4, 129.8, 129.6, 129.6, 128.3, 122.4, 121.9, 121.6, 120.2 (q, J = 255.8 Hz), 118.5, 24.2. HRMS (ESI+) m/z calcd for $\text{C}_{18}\text{H}_{14}\text{ClF}_3\text{N}_5\text{O}_2$ [$\text{M} + \text{H}$] $^+$ 424.0783, found 424.0780. HPLC purity: >99%, retention time = 14.1 min.

4-Chloro-6-(4-fluorophenyl)-N-(4-(trifluoromethoxy)phenyl)-1,3,5-triazin-2-amine (9b). The title compound was prepared from compound 11a and (4-fluorophenyl)boronic acid following the general procedure of 9a. White solid (30% yield). mp: 119.9–121.5 °C. ^1H NMR (400 MHz, DMSO- d_6): δ (ppm) 10.94 (s, 1H), 8.38 (s, 1H), 8.02–7.69 (m, 2H), 7.58–7.26 (m, 4H). ^{13}C NMR (101 MHz, DMSO- d_6): δ (ppm) 170.0, 167.0, 164.5, 144.5, 137.6, 131.8, 131.2, 122.6, 122.0, 120.6 (q, J = 255.6 Hz), 116.5, 116.3. HRMS (ESI+) m/z calcd for $\text{C}_{16}\text{H}_{10}\text{ClF}_4\text{N}_4\text{O}$ [$\text{M} + \text{H}$] $^+$ 385.0474, found 385.0467. HPLC purity: 96.3%, retention time = 14.8 min.

4-Chloro-6-(4-chlorophenyl)-N-(4-(trifluoromethoxy)phenyl)-1,3,5-triazin-2-amine (9c). The title compound was prepared from compound 11a and (4-chlorophenyl)boronic acid following the general procedure of 9a. White solid (22% yield). mp: 155.7–157.0 °C. ^1H NMR (400 MHz, CDCl $_3$): δ (ppm) 8.35 (d, J = 8.7 Hz, 1H), 7.66 (d, J = 9.0 Hz, 1H), 7.55 (s, 1H), 7.46 (d, J = 8.5 Hz, 1H), 7.28 (d, J = 8.3 Hz, 1H). ^{13}C NMR (101 MHz, CDCl $_3$): δ (ppm) 164.6, 145.9, 145.9, 139.9, 139.9, 135.6, 132.9, 130.6, 129.2, 122.2, 122.0, 120.6 (q, J = 258.1 Hz). HRMS (ESI+) m/z calcd for $\text{C}_{16}\text{H}_{10}\text{Cl}_2\text{F}_3\text{N}_4\text{O}$ [$\text{M} + \text{H}$] $^+$ 401.0178, found 401.0181. HPLC purity: 99.6%, retention time = 16.3 min.

4-Chloro-6-(4-methoxyphenyl)-N-(4-(trifluoromethoxy)phenyl)-1,3,5-triazin-2-amine (9d). The title compound was prepared from compound 11a and (4-methoxyphenyl)boronic acid following the general procedure of 9a. White solid (39% yield). mp: 164.8–166.3 °C. ^1H NMR (600 MHz, CDCl $_3$): δ (ppm) 8.39 (d, J = 8.6 Hz, 2H), 7.68 (d, J = 7.4 Hz, 2H), 7.45 (s, 1H), 7.27 (d, J = 10.3 Hz, 2H), 6.99 (d, J = 8.4 Hz, 2H), 3.89 (s, 3H). ^{13}C NMR (151 MHz, CDCl $_3$): δ (ppm) 173.1, 170.9, 164.5, 164.1, 145.7, 145.7, 136.0, 131.4, 126.9, 123.2, 120.6 (q, J = 257.1 Hz), 114.2, 55.7. HRMS (ESI+) m/z calcd for $\text{C}_{17}\text{H}_{13}\text{ClF}_3\text{N}_4\text{O}_2$ [$\text{M} + \text{H}$] $^+$ 397.0674, found 397.0675. HPLC purity: >99%, retention time = 15.5 min.

4-Chloro-6-(3-methoxyphenyl)-N-(4-(trifluoromethoxy)phenyl)-1,3,5-triazin-2-amine (9e). The title compound was prepared from compound 11a and (3-methoxyphenyl)boronic acid following the general procedure of 9a. White solid (54% yield). mp: 132.7–133.6 °C. ^1H NMR (400 MHz, DMSO- d_6): δ (ppm) 10.92 (s, 1H), 7.93–7.68 (m, 4H), 7.55–7.35 (m, 3H), 7.21 (d, J = 9.6 Hz, 1H), 3.83 (s, 3H). ^{13}C NMR (101 MHz, DMSO- d_6): δ (ppm) 169.7, 164.1, 159.4, 144.2, 137.2, 135.6, 130.0, 122.5, 122.3, 121.6, 121.4, 121.0, (q, J = 255.8 Hz), 119.4, 113.0, 55.1. HRMS (ESI+) m/z calcd for $\text{C}_{17}\text{H}_{13}\text{ClF}_3\text{N}_4\text{O}_2$ [$\text{M} + \text{H}$] $^+$ 397.0674, found 397.0674. HPLC purity: 95.9%, retention time = 15.6 min.

4-Chloro-6-(2-methoxyphenyl)-N-(4-(trifluoromethoxy)phenyl)-1,3,5-triazin-2-amine (9f). The title compound was prepared from compound 11a and (2-methoxyphenyl)boronic acid following the general procedure of 9a. White solid (64% yield). mp: 178.4–179.5 °C. ^1H NMR (400 MHz, DMSO- d_6): δ (ppm) 10.80 (s, 1H), 8.30 (d, J = 8.9 Hz, 2H), 7.84 (d, J = 32.1 Hz, 2H), 7.41 (d, J = 8.3 Hz, 2H), 7.10 (d, J = 8.9 Hz, 2H), 3.86 (s, 3H). ^{13}C NMR (101 MHz, DMSO- d_6): δ (ppm) 171.9, 169.5, 164.0, 163.5, 144.0, 137.4, 130.8, 130.6, 126.4, 122.3, 122.0, 121.6, 120.1 (q, J = 255.7 Hz), 114.2, 55.5. HRMS (ESI+) m/z calcd for $\text{C}_{17}\text{H}_{13}\text{ClF}_3\text{N}_4\text{O}_2$ [$\text{M} + \text{H}$] $^+$ 397.0674, found 397.0674. HPLC purity: 96.3%, retention time = 12.3 min.

4-Chloro-N,6-bis(4-methoxyphenyl)-1,3,5-triazin-2-amine (9g). The title compound was prepared from compound 11b and (4-methoxyphenyl)boronic acid following the general procedure of 9a. White solid (55% yield). mp: 177.5–178.8 °C. ^1H NMR (400 MHz, CDCl $_3$): δ (ppm) 8.37 (d, J = 8.7 Hz, 2H), 7.51 (s, 2H), 7.40 (s, 1H), 6.96 (d, J = 8.7 Hz, 4H), 3.88 (s, 3H), 3.83 (s, 3H). ^{13}C NMR (101 MHz, CDCl $_3$): δ (ppm) 173.0, 164.6, 163.9, 157.0, 131.4, 130.2, 127.6, 123.0, 114.1, 110.1, 55.7, 55.6. HRMS (ESI+) m/z calcd for $\text{C}_{17}\text{H}_{16}\text{ClN}_4\text{O}_2$ [$\text{M} + \text{H}$] $^+$ 343.0956, found 343.0956. HPLC purity: 97.5%, retention time = 19.8 min.

4-Chloro-6-(4-methoxyphenyl)-N-(4-(trifluoromethyl)phenyl)-1,3,5-triazin-2-amine (9h). The title compound was prepared from compound 11c and (4-methoxyphenyl)boronic acid following the general procedure of 9a. White solid (48% yield). mp: 177.9–178.8 °C. ^1H NMR (400 MHz, CDCl $_3$): δ (ppm) 8.39 (d, J = 8.9 Hz, 2H), 7.79 (d, J = 8.5 Hz, 2H), 7.66 (d, J = 8.5 Hz, 2H), 7.59 (s, 1H), 6.99 (d, J = 8.9 Hz, 2H), 3.89 (s, 3H). ^{13}C NMR (151 MHz, CDCl $_3$): δ (ppm) 173.1, 171.0, 164.5, 164.2, 140., 131.5, 126.8, 126.6 (q, J = 3.7 Hz), 126.3 (d, J = 32.9 Hz), 124.2 (q, J = 271.5 Hz), 120.3, 114.3, 55.7. HRMS (ESI+) m/z calcd for $\text{C}_{17}\text{H}_{13}\text{ClF}_3\text{N}_4\text{O}$ [$\text{M} + \text{H}$] $^+$ 381.0725, found 381.0724. HPLC purity: 95.0%, retention time = 21.3 min.

4-Chloro-6-(4-methoxyphenyl)-N-(p-tolyl)-1,3,5-triazin-2-amine (9i). The title compound was prepared from compound 11d and (4-methoxyphenyl)boronic acid following the general procedure of 9a. White solid (54% yield). mp: 177.1–177.9 °C. ^1H NMR (600 MHz, CDCl $_3$): δ (ppm) 8.39 (d, J = 8.4 Hz, 2H), 7.51 (s, 2H), 7.35 (s, 1H), 7.21 (d, J = 5.5 Hz, 2H), 6.98 (d, J = 8.9 Hz, 2H), 3.89 (s, 3H), 2.37 (s, 3H). ^{13}C NMR (151 MHz, CDCl $_3$): δ (ppm) 173.0, 170.5, 164.5, 163.9, 134.7, 134.6, 131.4, 129.8, 127.2, 121.1, 114.1, 55.6, 21.1. HRMS (ESI+) m/z calcd for $\text{C}_{17}\text{H}_{16}\text{ClN}_4\text{O}$ [$\text{M} + \text{H}$] $^+$ 327.1007, found 327.1005. HPLC purity: 96.1%, retention time = 20.6 min.

4-Chloro-6-(4-methoxyphenyl)-N-(3-(trifluoromethoxy)phenyl)-1,3,5-triazin-2-amine (9j). The title compound was prepared from compound 11e and (4-methoxyphenyl)boronic acid following the general procedure of 9a. White solid (52% yield). mp: 132.1–132.8 °C. ^1H NMR (400 MHz, CDCl $_3$): δ (ppm) 8.40 (d, J = 8.8 Hz, 2H), 7.91 (s, 1H), 7.43 (dd, J = 28.1, 20.3 Hz, 3H), 7.03 (d, J = 7.3 Hz, 1H), 6.99 (d, J = 8.9 Hz, 2H), 3.90 (s, 3H). ^{13}C NMR (151 MHz, CDCl $_3$): δ (ppm) 173.2, 170.9, 164.4, 164.2, 149.8, 138.8, 131.5, 130.3, 126.8, 120.64 (q, J = 257.6 Hz), 118.6, 116.7, 114.2, 113.5, 55.7. HRMS (ESI+) m/z calcd for $\text{C}_{17}\text{H}_{13}\text{ClF}_3\text{N}_4\text{O}_2$ [$\text{M} + \text{H}$] $^+$ 397.0674, found 397.0674. HPLC purity: >99%, retention time = 21.4 min.

4-(4-Methoxyphenyl)-6-methyl-N-(4-(trifluoromethoxy)phenyl)-1,3,5-triazin-2-amine (10a). Compound 9d (237 mg, 0.6 mmol) was treated with dimethyl zinc (63 mg, 0.6 mmol) in the presence of Pd(PPh $_3$) $_2\text{Cl}_2$ (14 mg, 0.02 mmol) in 1,4-dioxane (4 mL) for 6–9 h at 100 °C. Then cooled and the reaction mixture was concentrated under reduced pressure. The crude material was purified by silica gel chromatography (PE/EA = 15:1) to afford compound 10a. Brown solid (65% yield). mp: 144.1–144.9 °C. ^1H NMR (400 MHz, CDCl $_3$): δ (ppm) 8.42 (d, J = 8.8 Hz, 2H), 7.72 (d, J = 9.0 Hz, 2H), 7.41 (s, 1H), 7.24 (d, J = 8.8 Hz, 2H), 6.99 (d, J = 8.8 Hz, 2H), 3.89 (s, 3H), 2.57 (s, 3H). ^{13}C NMR (151 MHz, CDCl $_3$): δ (ppm) 175.7, 171.0, 163.8, 162.9, 145.3, 136.6, 131.2, 127.7, 121.9, 121.7, 120.7 (q, J = 256.9 Hz), 114.2, 55.6, 25.5. HRMS (ESI+) m/z calcd for $\text{C}_{18}\text{H}_{15}\text{F}_3\text{N}_4\text{O}_2$ [$\text{M} + \text{H}$] $^+$ 378.1174, found 378.1172. HPLC purity: 99.7%, retention time = 12.3 min.

4-Ethyl-6-(4-methoxyphenyl)-N-(4-(trifluoromethoxy)phenyl)-1,3,5-triazin-2-amine (10b). The title compound was prepared from compound **9d** and diethylzinc following the general procedure of **10a**. Brown solid (58% yield). mp: 108.9–109.9 °C. ¹H NMR (400 MHz, CDCl₃): δ (ppm) 8.43 (d, *J* = 8.9 Hz, 2H), 7.74 (d, *J* = 9.0 Hz, 2H), 7.38 (s, 1H), 7.24 (d, *J* = 8.7 Hz, 2H), 7.00 (d, *J* = 11.6 Hz, 2H), 3.89 (s, 3H), 2.83 (q, *J* = 7.6 Hz, 2H), 1.39 (t, *J* = 7.6 Hz, 3H). ¹³C NMR (151 MHz, CDCl₃): δ (ppm) 180.7, 171.2, 164.2, 163.3, 144.8, 137.3, 130.8, 128.6, 121.9, 121.2, 120.7 (q, *J* = 256.7 Hz), 114.0, 55.6, 32.4, 11.7. HRMS (ESI+) *m/z* calcd for C₁₉H₁₇F₃N₄O₂ [M + H]⁺ 391.1376, found 391.1370. HPLC purity: >99%, retention time = 14.1 min.

4-(4-Methoxyphenyl)-6-propyl-N-(4-(trifluoromethoxy)phenyl)-1,3,5-triazin-2-amine (10c). The title compound was prepared from compound **9d** and dipropylzinc following the general procedure of **10a**. White solid (53% yield). mp: 84.8–85.8 °C. ¹H NMR (400 MHz, CDCl₃): δ (ppm) 8.44 (d, *J* = 8.7 Hz, 2H), 7.75 (d, *J* = 8.9 Hz, 2H), 7.41 (s, 1H), 7.26 (d, *J* = 13.8 Hz, 2H), 7.01 (d, *J* = 8.7 Hz, 2H), 3.90 (s, 3H), 2.79 (t, *J* = 7.6 Hz, 2H), 1.99–1.86 (m, 2H), 1.06 (t, *J* = 7.4 Hz, 3H). ¹³C NMR (101 MHz, CDCl₃): δ (ppm) 179.8, 171.1, 164.2, 163.2, 144.8, 137.3, 130.7, 128.6, 121.8, 121.1, 120.7 (q, *J* = 256.9 Hz), 114.0, 55.5, 41.1, 21.0, 14.0. HRMS (ESI+) *m/z* calcd for C₂₀H₁₉F₃N₄O₂ [M + H]⁺ 405.1524, found 405.1527. HPLC purity: >99%, retention time = 14.5 min.

6-(4-Methoxyphenyl)-N²-(4-(trifluoromethoxy)phenyl)-1,3,5-triazine-2,4-diamine (10d). Compound **9d** (237 mg, 0.6 mmol) and NH₄Cl (37 mg, 0.7 mmol) were dissolved in THF (5 mL). Then, K₂CO₃ (97 mg, 0.7 mmol) was added and the reaction was held at 65 °C overnight with stirring. The reaction mixture was concentrated under reduced pressure. Then, water was added and quenched with ethanol. The crude material was purified by silica gel chromatography (PE/EA = 15:1) to afford compound **10d**. The title compound was prepared from compound **9d** and ammonia following the general procedure of **10a** as a white solid in a 60% yield. mp: 171.4–172.4 °C (reference melting point: 163–165 °C³⁴). ¹H NMR (400 MHz, CDCl₃): δ (ppm) 8.31 (d, *J* = 8.9 Hz, 2H), 7.62 (d, *J* = 9.0 Hz, 2H), 7.56 (s, 1H), 7.17 (d, *J* = 8.5 Hz, 2H), 6.96 (d, *J* = 9.0 Hz, 2H), 5.48 (s, 2H), 3.86 (s, 3H). ¹³C NMR (151 MHz, DMSO-*d*₆): δ (ppm) 170.0, 167.0, 164.5, 162.1, 142.6, 139.4, 129.7, 128.9, 121.3, 120.9, 120.24 (q, *J* = 255.2 Hz), 113.7, 55.3. HRMS (ESI+) *m/z* calcd for C₁₇H₁₄F₃N₅O [M + H]⁺ 378.1172, found 378.1174. HPLC purity: 99.6%, retention time = 15.8 min.

6-(4-Methoxyphenyl)-N²-methyl-N⁴-(4-(trifluoromethoxy)phenyl)-1,3,5-triazine-2,4-diamine (10e). Compound **9d** (237 mg, 0.6 mmol) and methanamine (70 mg, 0.7 mmol) were dissolved in THF (5 mL). Then, K₂CO₃ (97 mg, 0.7 mmol) was added and the reaction was held at 65 °C overnight with stirring. The reaction mixture was concentrated under reduced pressure. Then, water was added and quenched with ethanol. The crude material was purified by silica gel chromatography (PE/EA = 15:1) to afford compound **10e** as a white solid in a 52% yield. mp: 147.3–147.8 °C. ¹H NMR (400 MHz, DMSO-*d*₆): δ (ppm) 9.43 (s, 1H), 8.31 (d, *J* = 8.2 Hz, 2H), 7.95 (d, *J* = 9.0 Hz, 2H), 7.27 (d, *J* = 8.6 Hz, 2H), 7.21 (s, 1H), 7.08–6.88 (m, 2H), 3.85 (s, 3H), 2.95 (s, 3H). ¹³C NMR (151 MHz, DMSO-*d*₆): δ (ppm) 169.3, 166.0, 164.0, 161.9, 142.6, 139.0, 129.3, 128.9, 120.7, 120.6, 119.9 (q, *J* = 255.3 Hz), 113.4, 55.0, 26.9. HRMS (ESI+) *m/z* calcd for C₁₈H₁₆F₃N₅O₂ [M + H]⁺ 392.1329, found 392.1335. HPLC purity: 98.2%, retention time = 16.6 min.

6-(4-Methoxyphenyl)-N²-propyl-N⁴-(4-(trifluoromethoxy)phenyl)-1,3,5-triazine-2,4-diamine (10f). The title compound was prepared from compound **9d** and propan-1-amine following the general procedure of **10e**. White solid (55% yield). mp: 143.8–144.8 °C. ¹H NMR (400 MHz, DMSO-*d*₆): δ (ppm) 9.40 (s, 1H), 8.30 (d, *J* = 8.7 Hz, 2H), 8.04–7.84 (m, 2H), 7.35 (s, 1H), 7.27 (d, *J* = 8.6 Hz, 2H), 7.11–6.94 (m, 2H), 3.85 (s, 3H), 3.08 (s, 2H), 1.81–1.41 (m, 2H), 0.95 (t, *J* = 7.4 Hz, 3H). ¹³C NMR (101 MHz, DMSO-*d*₆): δ (ppm) 169.3, 165.6, 164.0, 161.8, 142.5, 139.0, 129.3, 128.9, 120.7, 120.5, 119.9 (q, *J* = 255.3 Hz), 113.3, 55.0, 41.8, 21.9, 10.9. HRMS (ESI+) *m/z* calcd for C₂₀H₂₀F₃N₅O₂ [M + H]⁺ 420.1642, found 420.1635. HPLC purity: 99.2%, retention time = 14.1 min.

N²-Benzyl-6-(4-methoxyphenyl)-N⁴-(4-(trifluoromethoxy)phenyl)-1,3,5-triazine-2,4-diamine (10g). The title compound was prepared from compound **9d** and phenylmethanamine following the general procedure of **10e**. White solid (49% yield). mp: 143.2–144.2 °C. ¹H NMR (400 MHz, CDCl₃): δ (ppm) 8.35 (d, *J* = 7.4 Hz, 2H), 7.59 (d, *J* = 7.6 Hz, 2H), 7.47 (s, 1H), 7.39–7.26 (m, 5H), 7.13 (m, 2H), 6.95 (d, *J* = 7.0 Hz, 2H), 5.91 (s, 1H), 4.71 (s, 2H), 3.86 (s, 3H). ¹³C NMR (151 MHz, CDCl₃): δ (ppm) 171.0, 166.4, 164.6, 162.8, 144.4, 138.6, 137.7, 130.2, 128.8, 127.9, 127.4, 121.7, 121.5, 121.1, 120.68 (q, *J* = 256.5 Hz), 113.8, 55.5, 45.1. HRMS (ESI+) *m/z* calcd for C₂₄H₂₀F₃N₅O₂ [M + H]⁺ 468.1642, found 468.1638. HPLC purity: >99%, retention time = 15.5 min.

6-(4-Methoxyphenyl)-N²-methyl-N⁴-phenyl-N⁴-(4-(trifluoromethoxy)phenyl)-1,3,5-triazine-2,4-diamine (10h). The title compound was prepared from compound **9d** and *N*-methylaniline following the general procedure of **10e**. White solid (42% yield). mp: 132.1–133.2 °C. ¹H NMR (400 MHz, CDCl₃): δ (ppm) 8.35 (s, 2H), 7.48 (s, 2H), 7.45 (s, 1H), 7.44–7.27 (m, 5H), 7.03 (d, *J* = 8.8 Hz, 2H), 6.96 (d, *J* = 8.6 Hz, 2H), 3.87 (s, 3H), 3.66 (s, 3H). ¹³C NMR (151 MHz, CDCl₃): δ (ppm) 170.6, 165.8, 163.8, 162.8, 144.5, 137.9, 130.4, 129.1, 128.9, 127.1, 126.4, 121.5, 121.2, 120.8 (q, *J* = 307.5 Hz), 120.4, 113.8, 55.5, 38.0. HRMS (ESI+) *m/z* calcd for C₂₄H₂₀F₃N₅O₂ [M + H]⁺ 468.1642, found 468.1641. HPLC purity: 99.2%, retention time = 21.7 min.

4-(4-Methoxyphenyl)-6-(4-methylpiperazin-1-yl)-N-(4-(trifluoromethoxy)phenyl)-1,3,5-triazin-2-amine (10i). The title compound was prepared from compound **9d** and 1-methylpiperazine following the general procedure of **10e**. White solid (55% yield). mp: 180.2–180.7 °C. ¹H NMR (400 MHz, CDCl₃): δ (ppm) 8.35 (d, *J* = 8.8 Hz, 2H), 7.65 (d, *J* = 8.9 Hz, 2H), 7.20 (d, *J* = 8.7 Hz, 2H), 7.14 (s, 1H), 6.97 (d, *J* = 8.8 Hz, 2H), 4.00 (d, *J* = 40.4 Hz, 4H), 3.88 (s, 3H), 2.55 (s, 4H), 2.39 (s, 3H). ¹³C NMR (151 MHz, CDCl₃): δ (ppm) 170.8, 165.0, 164.5, 162.8, 144.3, 138.0, 130.3, 129.4, 121.8, 120.9, 120.7 (q, *J* = 256.5 Hz), 113.7, 55.5, 55.0, 46.2, 43.2. HRMS (ESI+) *m/z* calcd for C₂₂H₂₄F₃N₆O₂ [M + H]⁺ 461.1907, found 461.1906. HPLC purity: 99.7%, retention time = 20.4 min.

4-(4-Methoxyphenyl)-6-morpholino-N-(4-(trifluoromethoxy)phenyl)-1,3,5-triazin-2-amine (10j). The title compound was prepared from compound **9d** and morpholine following the general procedure of **10e**. White solid (56% yield). mp: 191.2–191.7 °C. ¹H NMR (400 MHz, CDCl₃): δ (ppm) 8.35 (d, *J* = 8.9 Hz, 2H), 7.64 (d, *J* = 9.0 Hz, 2H), 7.30 (s, 1H), 7.19 (d, *J* = 8.6 Hz, 2H), 6.96 (d, *J* = 11.7 Hz, 2H), 4.10–3.73 (m, 11H). ¹³C NMR (151 MHz, DMSO-*d*₆): δ (ppm) 169.6, 164.6, 164.1, 162.3, 142.8, 142.8, 139.2, 129.9, 121.4, 120.9, 120.2 (q, *J* = 255.2 Hz), 113.7, 66.0, 55.4, 43.5. HRMS (ESI+) *m/z* calcd for C₂₁H₂₀F₃N₅O₃ [M + H]⁺ 448.1591, found 448.1586. HPLC purity: 99.5%, retention time = 20.9 min.

2-(4-(4-(4-Methoxyphenyl)-6-((4-(trifluoromethoxy)phenyl)-amino)-1,3,5-triazin-2-yl)piperazin-1-yl)ethan-1-ol (10k). The title compound was prepared from compound **9d** and 2-(piperazin-1-yl)ethan-1-ol following the general procedure of **10e**. White solid (43% yield). mp: 148.1–149.3 °C. ¹H NMR (400 MHz, CDCl₃): δ (ppm) 8.35 (d, *J* = 8.8 Hz, 2H), 7.64 (d, *J* = 8.9 Hz, 2H), 7.29 (s, 1H), 7.19 (d, *J* = 8.6 Hz, 2H), 6.96 (d, *J* = 8.9 Hz, 2H), 4.11–3.90 (m, 4H), 3.87 (s, 3H), 3.69 (t, *J* = 5.2 Hz, 2H), 2.77 (s, 1H), 2.61 (dd, *J* = 8.9, 4.5 Hz, 6H). ¹³C NMR (101 MHz, CDCl₃): δ (ppm) 170.7, 164.9, 164.4, 162.6, 144.2, 137.9, 130.2, 129.3, 121.6, 120.7, 120.6 (d, *J* = 256.5 Hz), 113.6, 59.5, 57.8, 55.4, 52.8, 43.4. HRMS (ESI+) *m/z* calcd for C₂₃H₂₅F₃N₆O₃ [M + H]⁺ 491.2013, found 491.2019. HPLC purity: 98.2%, retention time = 19.1 min.

4-(4-Methoxyphenyl)-6-(prop-1-yn-1-yl)-N-(4-(trifluoromethoxy)phenyl)-1,3,5-triazin-2-amine (10l). Compound **9d** (325 mg, 1.0 mmol), prop-1-yne (80 mg, 2 mmol), Pd(PPh₃)₂Cl₂ (28 mg, 0.04 mmol), CuTC (38 mg, 0.2 mmol), CuI (38 mg, 0.2 mmol), dppp (16 mg, 2 mmol), K₂CO₃ (276 mg, 2.0 mmol), and THF (5 mL) were added in 35 mL sealed tubes in turn. Then, the reaction mixture was held at 95 °C for 15 h with stirring under the protection of argon. After the reaction was completed, EA (50 mL) was added and the mixture was filtered through celite. The mixture was concentrated under reduced pressure. The crude material was

purified by silica gel chromatography (PE/EA = 20:1) to afford compound **10l** as a brown solid in 35% yield. mp: 159.4–160.1 °C. ¹H NMR (400 MHz, CDCl₃): δ (ppm) 8.40 (d, *J* = 8.3 Hz, 2H), 7.87 (s, 1H), 7.71 (d, *J* = 8.3 Hz, 2H), 7.25 (d, *J* = 9.3 Hz, 2H), 6.98 (d, *J* = 8.3 Hz, 2H), 3.88 (s, 3H), 2.06 (s, 3H). ¹³C NMR (151 MHz, CDCl₃): δ (ppm) 171.7, 163.9, 163.7, 160.4, 145.2, 136.7, 131.0, 127.8, 121.9, 121.8, 120.7 (q, *J* = 256.8 Hz), 114.1, 89.1, 78.8, 55.6, 4.6. HRMS (ESI+) *m/z* calcd for C₂₀H₁₃F₃N₄O₂ [M + H]⁺ 401.1220, found 401.1216. HPLC purity: 98.1%, retention time = 14.1 min.

4-(4-Methoxyphenyl)-6-(*p*-tolylethynyl)-*N*-(4-(trifluoromethoxy)phenyl)-1,3,5-triazin-2-amine (10m). The title compound was prepared from compound **9d** and 1-ethynyl-4-methylbenzene following the general procedure of **10l**. Brown solid (41% yield). mp: 158.9–159.9 °C. ¹H NMR (400 MHz, CDCl₃): δ (ppm) 8.45 (d, *J* = 8.8 Hz, 2H), 7.92 (s, 1H), 7.75 (d, *J* = 8.9 Hz, 2H), 7.52 (d, *J* = 7.1 Hz, 2H), 7.24 (d, *J* = 8.4 Hz, 2H), 7.18 (d, *J* = 7.7 Hz, 2H), 7.00 (d, *J* = 8.8 Hz, 2H), 3.89 (s, 3H), 2.39 (s, 3H). ¹³C NMR (151 MHz, CDCl₃): δ (ppm) 176.7, 175.7, 164.0, 163.0, 145.4, 141.2, 136.4, 136.4, 133.2, 131.3, 129.5, 122.0, 121.9, 120.7 (q, *J* = 257.0 Hz), 117.7, 114.3, 91.6, 90.1, 55.7, 21.9. HRMS (ESI+) *m/z* calcd for C₂₆H₁₉F₃N₄O₂ [M + H]⁺ 477.1533, found 477.1530. HPLC purity: 99.4%, retention time = 12.7 min.

4,6-Dichloro-*N*-(4-(trifluoromethoxy)phenyl)aniline (11a). 2,4,6-Trichloro-[1,3,5]triazine (1.917 g, 10.4 mmol) was dissolved in anhydrous THF (15 mL), and a solution of 4-(trifluoromethoxy)aniline (1.911 g, 10.8 mmol) and Et₃N (1.088 g, 10.8 mmol) in THF (7 mL) was added under ice bath. Then, the reaction was held at room temperature overnight with stirring. The reaction mixture was concentrated under reduced pressure. Then, water was added and quenched with ethanol. The crude material was purified by silica gel chromatography (PE/EA = 20:1) to afford compound **11a** as a white solid in a 57% yield. mp: 137.1–138.7 °C (reference melting point: 119.0–122.0 °C³⁵). ¹H NMR (400 MHz, CDCl₃): δ (ppm) 7.79 (s, 1H), 7.59 (d, *J* = 9.0 Hz, 2H), 7.27 (d, *J* = 8.6 Hz, 2H). ¹³C NMR (101 MHz, CDCl₃): δ (ppm) 171.7, 170.6, 164.3, 146.6, 134.5, 122.9, 122.1, 120.4 (q, *J* = 257.6 Hz).

4,6-Dichloro-*N*-(4-methoxyphenyl)aniline (11b). The title compound was prepared from 2,4,6-trichloro-[1,3,5]triazine and 4-methoxyaniline following the general procedure of compound **11a**. White solid (48% yield). mp: 174.9–176.5 °C (reference melting point: 167.0–169.5 °C³⁶). ¹H NMR (400 MHz, CDCl₃): δ (ppm) 7.61 (s, 1H), 7.41 (d, *J* = 9.0 Hz, 2H), 6.93 (d, *J* = 9.0 Hz, 2H), 3.82 (s, 3H). ¹³C NMR (101 MHz, CDCl₃): δ (ppm) 171.5, 170.2, 164.4, 157.9, 128.5, 123.7, 114.6, 55.7.

4,6-Dichloro-*N*-(4-(trifluoromethyl)phenyl)aniline (11c). The title compound was prepared from 2,4,6-trichloro-[1,3,5]triazine and 4-(trifluoromethyl)aniline following the general procedure of compound **11a**. White solid (20% yield). mp: 159.0–160.1 °C (reference melting point: 158.0–161.0 °C³⁷). ¹H NMR (400 MHz, CDCl₃): δ (ppm) 7.78 (s, 1H), 7.71 (d, *J* = 8.8 Hz, 2H), 7.67 (d, *J* = 8.9 Hz, 2H). ¹³C NMR (101 MHz, CDCl₃): δ (ppm) 164.3, 139.0, 127.7, 126.7, 126.7, 123.9 (q, *J* = 271.7 Hz), 121.0.

4,6-Dichloro-*N*-(*p*-tolyl)aniline (11d). The title compound was prepared from 2,4,6-trichloro-[1,3,5]triazine and *p*-toluidine following the general procedure of compound **11a**. White solid (27% yield). mp: 130.1–131.8 °C (reference melting point: 162.0–162.5 °C³⁸). ¹H NMR (400 MHz, CDCl₃): δ (ppm) 7.70 (s, 1H), 7.39 (d, *J* = 8.5 Hz, 2H), 7.20 (d, *J* = 8.2 Hz, 2H), 2.35 (s, 3H). ¹³C NMR (101 MHz, CDCl₃): δ (ppm) 171.42, 170.24, 171.42, 164.2, 136.0, 133.1, 129.9, 121.7, 21.1.

4,6-Dichloro-*N*-(3-(trifluoromethoxy)phenyl)aniline (11e). The title compound was prepared from 2,4,6-trichloro-[1,3,5]triazine and 3-(trifluoromethoxy)aniline following the general procedure of compound **11a**. White solid (35% yield). mp: 128.1–129.8 °C. ¹H NMR (400 MHz, CDCl₃): δ (ppm) 7.48 (ddd, *J* = 30.5, 20.7, 8.1 Hz, 3H), 7.19 (d, *J* = 8.0 Hz, 1H), 7.14 (s, 1H). ¹³C NMR (101 MHz, CDCl₃): δ (ppm) 172.4, 167.7, 149.8, 139.2, 131.3, 126.9, 122.0, 121.5, 120.5 (q, *J* = 259.6 Hz), 108.0.

Two-Electrode Voltage Clamp (TEVC) Recording in *Xenopus* Oocytes. Oocytes were harvested from *X. laevis* female clawed frogs

after anesthesia, washed twice in the Ca²⁺-free OR2 solution (82.5 mM NaCl, 2.5 mM KCl, 1 mM MgCl₂, 5 mM 4-(2-hydroxyethyl)-1-piperazineethanesulfonic acid (HEPES), pH 7.4) before transferred to ~25 mL tubes, and treated with 2 mg/mL collagenase in OR2 solution (Sigma type II, Sigma-Aldrich, Inc., St. Louis, MO) for 20 min at 20–25 °C under gentle rotation. The stage V and VI oocytes were selected for microinjections. For two-electrode voltage clamp recordings in oocytes, capped cRNAs were transcribed *in vitro* using the T3 mMESSAGEMACHINE Kit (Ambion, Austin, TX) following the linearization of plasmids in pBluescript KSM vectors. The oocytes were injected with 46 nL of cRNA solution containing approximately 20 ng human α7 nAChR cRNA or approximately 1 ng human 5-HT_{3A} cRNA using a microinjector (Drummond Scientific, Broomall, PA). For the expression of heteromeric rat α3β4 and rat α4β2 nAChRs, approximately 2 ng total cRNAs were injected in a 1:1 combination of each subunit into oocytes that were incubated at 16 °C in ND96 solution (96 mM NaCl, 2 mM KCl, 1.8 mM CaCl₂, 1 mM MgCl₂, 5 mM 4-(2-hydroxyethyl)-1-piperazineethanesulfonic acid (HEPES), pH 7.4 adjusted with NaOH). Recordings were made 24–72 h post-injection. Oocytes were impaled with two micro-electrodes (0.5–1.0 MΩ) filled with 3 M KCl in a 40-μL recording chamber. The membrane potential was held at −90 mV using standard voltage clamp procedures. Currents were recorded in Ringer's solution (115 mM NaCl, 2.5 mM KCl, 10 mM HEPES, 1.8 mM CaCl₂, 1 mM MgCl₂, 0.0005 mM atropine) at room temperature (22 ± 1 °C) using a GeneClamp 500B amplifier (Axon Instruments, Union City, CA).

Culture and Whole-Cell Patch Clamp Recordings of HEK293 Cells Stably Expressing hERG Channel. Human embryonic kidney HEK 293 cells were stably transfected with hERG cDNA, passaged in Dulbecco's modified Eagle's medium supplemented with 10% fetal bovine serum, penicillin (100 U/mL), streptomycin (100 μg/mL), and geneticin (200 μg/mL), seeded on 8 mm × 8 mm glass coverslips in 35 mm² diameter dishes (containing 2 mL of medium) at a density that enabled the cells to be isolated for whole-cell voltage clamp recordings, and cultured at 37 °C in a humidified 5% CO₂ environment.

For whole-cell patch clamp recordings, currents were recorded at room temperature using an EPC 10 UBS patch clamp amplifier in combination with Patchmaster (HEKA). The total resistance of patch electrodes was measured to be 3–5 MΩ. The extracellular solution contained 140 mM, 4 mM KCl, 1.8 mM CaCl₂, 1 mM MgCl₂, 10 mM glucose, and 10 mM HEPES with pH adjusted to 7.4 with NaOH. The internal pipette solution contained 130 mM KCl, 1 mM MgCl₂, 5 mM ethylene glycol-bis(β-aminoethyl ether)-*N,N,N',N'*-tetraacetic acid (EGTA) salt, 5 mM MgATP, and 10 mM HEPES with pH adjusted to 7.2 with KOH. The cells were clamped from the holding potential at −80 to +20 mV for 2 s, before repolarization to −40 mV for 1.6 s, and then back to the holding potential. The voltage protocol was run once every 10 s. Data were acquired and analyzed using the PatchMaster software (HEKA).

Liquid Chromatography–Mass Spectrometry (LC-MS) Assay for Pharmacokinetic Analysis of 10e and 10d. The plasma concentration–time profile: each of compounds **10e** and **10d** in a formulation of DMSO/poly(ethylene glycol) (PEG)400/H₂O (10:50:40, v/v/v) solution was administered intravenously at dose of 1 mg/kg and administrated orally at dose of 3 mg/kg or administration intraperitoneally at dose of 3 mg/kg, respectively, after 0.033 (iv only), 0.083, 0.25, 0.5, 1, 2, 4, 8, and 24 h administration.

All plasma samples were stored at −20 °C before end point (24 h post-dose), then were transferred to −80 °C after the last sampling, and thawed at room temperature before use. A 200 μL mixture of internal standard (5 ng/mL terfenadine) in methanol/acetonitrile (1:1, v/v) was added to a 10 μL aliquot of each standard, QC, control blank, and unknown samples. A 200 μL aliquot of blank methanol/acetonitrile (1:1, v/v) was added to the double blank. The samples were mixed for 1 min and centrifuged at 4000 rpm at 4 °C for 15 min; then, the supernatant was transferred (5 μL for **10e** or 50 μL for **10d**) into a clean vial containing 200 μL of a mixture of methanol and water (1:1, v/v) containing 0.1% formic acid (FA), vortexed for

approximately 30 s. A certain amount of the sample (2 μL for **10e** or 10 μL for **10d**) was injected for LC-MS/MS analysis.

LC-MS/MS was performed on a Shimadzu HPLC system coupled to an API5500 detector (Sciex). All separations were performed on a Kinetex C18 100A column (3.0 mm \times 50 mm, 2.6 μm) at room temperature with a flow rate of 0.7 mL/min. Mobile phase A consisted of 0.1% formic acid in 5 mM ammonium acetate buffer, and mobile phase B consisted of 0.1% formic acid in acetonitrile. Chromatography used a linear gradient by maintaining 40% mobile phase B for 0.4 min, 40–95% mobile phase B over 1.8 min for **10e** or over 1.8 min for **10d**, followed by a 95% B wash for 0.5 min for **10e** or for 0.1 min for **10d**, and a reequilibration at 40% B for 0.7 min. The mass spectrometer was operated in positive-ion mode using an electrospray ionization (ESI) source. The multiple reaction monitoring (MRM) mode was used to detect the specific precursor ion to product ion transitions of m/z 392.25 \rightarrow 242.10 for **10e**, 379.19 \rightarrow 134.00 for **10d**, and 472.4 \rightarrow 436.4 for terfenadine (IS). The optimal ESI-MS/MS parameters were as follows: positive electrospray ionization with ion spray (IS) voltage of 4500 V, collision gas (CAD) of 10 psi, source temperature (TEM) of 550 $^{\circ}\text{C}$, nebulizer (gas 1) 55 psi, turbo ion (gas 2) of 60 psi, and curtain gas (CUR) 40 psi for **10e** and **10d**.

Data Analysis. Data collection was performed using Analyst Software version 1.6.1 from Sciex. The measured plasma concentration data for each test compound (**10e** or **10d**), the nominal sample collection time, and doses were used for PK analysis. The pharmacokinetic parameters of each test compound (**10e** or **10d**) were determined by noncompartmental analysis using WinNonlin (Phoenix Build 8.0.0.3176).

Pharmacokinetics of 10e in Plasma, Brain, and Cerebrospinal Fluid (CSF). The ability of **10e** to penetrate the blood–brain barrier (BBB) *in vivo* was determined by the HPLC-MS-MS analysis as described below. Compound **10e** was formulated in 10% DMSO/50% PEG400/40% H_2O as a 1.5 mg/mL solution for intraperitoneal administration with a dosing volume of 2 mL/kg. The plasma, brain, and CSF of the mice (three mice per timepoint) were collected at 0.5, 2, and 8 h post-dose.

All plasma samples were temporarily stored at $-20\text{ }^{\circ}\text{C}$ after sampling, then were transferred to $-80\text{ }^{\circ}\text{C}$ after the end point, and then were thawed at room temperature before use. A 200 μL mixture of internal standard (5 ng/mL terfenadine) in methanol/acetonitrile (1:1, v/v) was added to a 20 μL aliquot of each standard, QC, control blank, and unknown samples. A 200 μL aliquot of blank methanol/acetonitrile (1:1, v/v) was added to the double blank. The samples were mixed for 1 min, centrifuged at 4000 rpm at $4\text{ }^{\circ}\text{C}$ for 15 min, then transferred (10 μL of the supernatant) into a clean vial containing 200 μL of a mixture of methanol and water (1:1, v/v) containing 0.1% formic acid (FA), and vortexed for approximately 30 s. An 8 μL aliquot of the sample was injected for LC-MS/MS analysis.

All brain samples were temporarily stored at dry ice after sampling and then transferred to $-80\text{ }^{\circ}\text{C}$ after the last sampling timepoint. Brain samples were thawed at room temperature, then were homogenized with fourfold distilled water as weight as the brain (1:4, weight/volume). A 200 μL mixture of internal standard (5 ng/mL terfenadine) in methanol/acetonitrile (1:1, v/v) was added to a 50 μL aliquot of each standard, QC, control blank, and unknown homogenate samples. A 200 μL aliquot of blank methanol/acetonitrile (1:1, v/v) was added to the double blank. The samples were mixed for 1 min, centrifuged at 4000 rpm at $4\text{ }^{\circ}\text{C}$ for 15 min, then transferred (10 μL of the supernatant) into a clean vial containing 200 μL of a mixture of methanol and water (1:1, v/v) containing 0.1% formic acid (FA), and vortexed for approximately 30 s. A 2 μL aliquot of the sample was injected for LC-MS/MS analysis.

All CSF samples were temporarily stored at $-20\text{ }^{\circ}\text{C}$ after sampling, transferred to $-80\text{ }^{\circ}\text{C}$ after the end point, and then thawed at room temperature before use. A 200 μL mixture of internal standard (5 ng/mL terfenadine) in methanol/acetonitrile (1:1, v/v) was added to a 3 μL aliquot of each standard, QC, control blank, and unknown samples. A 200 μL aliquot of blank methanol/acetonitrile (1:1, v/v) was added to the double blank. The samples were mixed for 1 min

and centrifuged at 4000 rpm at $4\text{ }^{\circ}\text{C}$ for 15 min, transferred (50 μL of the supernatant) into a clean vial containing 100 μL of a mixture of methanol and water (1:1, v/v) containing 0.1% formic acid (FA), and vortexed for approximately 30 s. A 2 μL aliquot of the sample was injected for LC-MS/MS analysis.

LC-MS/MS was performed on a Shimadzu HPLC system coupled to an API4000 (Sciex) for plasma or an API5500 (Sciex) for brain and CSF detector. For plasma, all separations were performed on a Kinetex C18 EVO 100A column (2.1 mm \times 50 mm, 2.6 μm) at room temperature with a flow rate of 0.7 mL/min. Mobile phase A consisted of 0.1% formic acid in 5 mM ammonium acetate buffer, and mobile phase B consisted of 0.1% formic acid in acetonitrile. Chromatography used a linear gradient by maintaining 37% mobile phase B for 0.4 min, 37–95% mobile phase B over 1.6 min, followed by a 95% B wash for 0.2 min and a reequilibration at 37% B for 0.8 min. For brain and CSF, all separations were performed on a Kinetex C18 100A column (3.0 mm \times 50 mm, 2.6 μm) at room temperature with a flow rate of 0.7 mL/min. Mobile phase A consisted of 0.1% formic acid in 5 mM ammonium acetate buffer, and mobile phase B consisted of 0.1% formic acid in acetonitrile. Chromatography used a linear gradient by maintaining 40% mobile phase B for 0.4 min, 40–95% mobile phase B over 1.4 min, followed by a 95% B wash for 0.5 min and a reequilibration at 37% B for 0.7 min. The mass spectrometer was operated in positive-ion mode using an electrospray ionization (ESI) source. The multiple reaction monitoring (MRM) mode was used to detect the specific precursor ion to product ion transitions of m/z 392.25 \rightarrow 242.10 for **10e** and 472.40 \rightarrow 436.40 for terfenadine (IS). The optimal ESI-MS/MS parameters for plasma were as follows: positive electrospray ionization with ion spray (IS) voltage of 5500 V, collision gas (CAD) of 12 psi, source temperature (TEM) of 500 $^{\circ}\text{C}$, nebulizer (gas 1) 60 psi, turbo ion (gas 2) of 65 psi, and curtain gas (CUR) 25 psi. The optimal ESI-MS/MS parameters for brain were as follows: positive electrospray ionization with ion spray voltage (IS) of 4500 V, collision gas (CAD) of 10 psi, source temperature (TEM) of 550 $^{\circ}\text{C}$, nebulizer (gas 1) 55 psi, turbo ion (gas 2) of 60 psi, and curtain gas (CUR) 40 psi.

Data Analysis. Data collection was performed using Analyst Software version 1.6.3 from Sciex for plasma and Analyst Software version 1.6.1 from Sciex for both brain and CSF.

Prepulse Inhibition (PPI) Test. Adult C57BL/6J males ($n = 8$ –11 for each group) were group-housed (four to five per cage) in a temperature-controlled ($23 \pm 2\text{ }^{\circ}\text{C}$) and humidity-controlled ($50 \pm 5\%$) environment on a 12/12 h light/dark cycle (light 7:00 AM to 7:00 PM) with ad libitum access to food and water. The animal experimental protocols were approved by the Animal Use and Care Committee of Qingdao University and were consistent with the Ethical Guidelines of the International Association for Animal Welfare. Test (**10e**) and tool (MK-801) compounds were, respectively, diluted in 40% poly(ethylene glycol) (PEG) or 0.9% saline to desired concentrations 12 h before the experiments and stored at $-20\text{ }^{\circ}\text{C}$. The compound solutions of different concentrations were administered to mice intraperitoneally at 5 mL/kg body weight.

PPI was measured in four standard startle chambers. A mouse holder rested on the platform in each sound-attenuated chamber. The motor response was monitored with a vibration sensor on the platform connected to a computer and recorded using the PACKWIN 2.0 software. The mice were placed in the laboratory for at least 2 days before the test to adapt to the environment. One day before the test, the mice were habituated to the environment in a plexiglass cylinder for 15 min under 68 dB background noise. In the next day, following a 5 min acclimatization period with background noise (68 dB), the mice were exposed to 70 test trials including 10 pulse-only trials, 50 prepulse–pulse trials, and 10 null trials under 68 dB background noise. The pulse-only trial consisted of a single 40 ms 120 dB white noise burst. Prepulses of various intensities consisted of 4, 8, 12, 16, and 20 dB above the 68 dB background, respectively. The duration of prepulse stimuli was 20 ms. The interval of the prepulse and pulse stimuli on prepulse–pulse trials was 80 ms. Only white noise background was used as the stimulus for the null-only trials. All trials

were conducted in the pseudo-random order at the intervals ranging from 8 to 22 s with an average value of 15 s. The percent PPI for each prepulse intensity was calculated by applying the following formula: % PPI = $[1 - (\text{startle response for prepulse} + \text{startle trial}) / (\text{startle response for startle stimulus alone trial})] \times 100\%$. When the value is 0, there is no PPI, and the greater the value of PPI, the deeper the degree of inhibition.

Molecular Docking. The initial structures of ligands (**6** and **10e**) were drawn through Schrodinger 2018. The ligands' structures were then preprocessed by LigPrep (OPLS-2005 force fields) to generate the three-dimensional (3D) structures and assign the ionization state of the ligands to neutrality. So far, the 3D structure of human $\alpha 7$ nAChR has not been reported. Therefore, we use the refined open-state homology model reported by Newcombe et al. as the receptor for docking analysis. The Protein Preparation Wizard module processed protein structure in Maestro before docking analysis. The entire docking process was executed in Schrodinger 2018. The binding site between the subunits identified by Newcombe et al. was used as the docking site, and extra precision (XP) docking was used to obtain the binding mode of the studied system under the default parameters. The final complex conformations were determined by the docking score.

■ ASSOCIATED CONTENT

Supporting Information

The Supporting Information is available free of charge at <https://pubs.acs.org/doi/10.1021/acs.jmedchem.1c01058>.

Rat liver microsome stability assessment of test compounds; Individual concentrations of **9d** in rats dosed by IV at 1 mg/kg; Individual concentrations of **9d** in rats dosed by PO at 10 mg/kg; Individual concentrations of **10d** in mice dosed by IV at 1 mg/kg and PO/IP at 3 mg/kg; Individual concentrations of **10e** in mice dosed by IV at 1 mg/kg and PO/IP at 3 mg/kg; Selective increase on other subtypes by compound **8l**, **9d**, and **10e** instead of $\alpha 7$ nAChR current; Mean concentrations of **10e** in plasma and brain; NMR spectra, HPLC reports and HRMS of the target compounds **8–10** (PDF)

PAINS filter using False Positive Remover (PDF)

Molecular formula strings of the target compounds (CSV)

Docking results of compound **5b** with modeled human $\alpha 7$ nAChR (PDB)

Docking results of compound **10e** with modeled human $\alpha 7$ nAChR (PDB)

■ AUTHOR INFORMATION

Corresponding Authors

KeWei Wang – Department of Pharmacology, School of Pharmacy, Qingdao University Medical College, Qingdao 266073, China; Institute of Innovative Drugs, Qingdao University, Qingdao 266021, China; orcid.org/0000-0001-7023-9998; Phone: +86 532 82991070; Email: wangkw@qdu.edu.cn

Qi Sun – State Key Laboratory of Natural and Biomimetic Drugs, School of Pharmaceutical Sciences, Peking University, Beijing 100191, China; orcid.org/0000-0002-8764-5877; Phone: +86 10 82805549; Email: sunqi@bjmu.edu.cn

Authors

Xintong Wang – State Key Laboratory of Natural and Biomimetic Drugs, School of Pharmaceutical Sciences, Peking University, Beijing 100191, China; Department of Molecular

and Cellular Pharmacology, School of Pharmaceutical Sciences, Peking University, Beijing 100191, China

Haoran Xiao – State Key Laboratory of Natural and Biomimetic Drugs, School of Pharmaceutical Sciences, Peking University, Beijing 100191, China

Jing Wang – Department of Pharmacology, School of Pharmacy, Qingdao University Medical College, Qingdao 266073, China

Zongze Huang – State Key Laboratory of Natural and Biomimetic Drugs, School of Pharmaceutical Sciences, Peking University, Beijing 100191, China

Geng Peng – State Key Laboratory of Natural and Biomimetic Drugs, School of Pharmaceutical Sciences, Peking University, Beijing 100191, China

Wenjun Xie – State Key Laboratory of Natural and Biomimetic Drugs, School of Pharmaceutical Sciences, Peking University, Beijing 100191, China; Department of Molecular and Cellular Pharmacology, School of Pharmaceutical Sciences, Peking University, Beijing 100191, China

Xiling Bian – Department of Molecular and Cellular Pharmacology, School of Pharmaceutical Sciences, Peking University, Beijing 100191, China

Huijie Liu – Department of Pharmacology, School of Pharmacy, Qingdao University Medical College, Qingdao 266073, China

Cheng Shi – State Key Laboratory of Natural and Biomimetic Drugs, School of Pharmaceutical Sciences, Peking University, Beijing 100191, China

Taoyi Yang – Department of Molecular and Cellular Pharmacology, School of Pharmaceutical Sciences, Peking University, Beijing 100191, China

Xin Li – State Key Laboratory of Natural and Biomimetic Drugs, School of Pharmaceutical Sciences, Peking University, Beijing 100191, China

Jian Gao – Department of Molecular and Cellular Pharmacology, School of Pharmaceutical Sciences, Peking University, Beijing 100191, China

Ying Meng – State Key Laboratory of Natural and Biomimetic Drugs, School of Pharmaceutical Sciences, Peking University, Beijing 100191, China

Qianchen Jiang – State Key Laboratory of Natural and Biomimetic Drugs, School of Pharmaceutical Sciences, Peking University, Beijing 100191, China

Wei Chen – State Key Laboratory of Natural and Biomimetic Drugs, School of Pharmaceutical Sciences, Peking University, Beijing 100191, China

Fang Hu – Department of Pharmacology, School of Pharmacy, Qingdao University Medical College, Qingdao 266073, China

Ningning Wei – Department of Pharmacology, School of Pharmacy, Qingdao University Medical College, Qingdao 266073, China; Institute of Innovative Drugs, Qingdao University, Qingdao 266021, China

Xiaowei Wang – State Key Laboratory of Natural and Biomimetic Drugs, School of Pharmaceutical Sciences, Peking University, Beijing 100191, China

Liangren Zhang – State Key Laboratory of Natural and Biomimetic Drugs, School of Pharmaceutical Sciences, Peking University, Beijing 100191, China; orcid.org/0000-0002-7362-9497

Complete contact information is available at: <https://pubs.acs.org/doi/10.1021/acs.jmedchem.1c01058>

Author Contributions

X.W., H.X., and J.W. contributed equally to this work. The manuscript was written through contributions of all authors.

Notes

The authors declare no competing financial interest.

ACKNOWLEDGMENTS

The project was supported by the funds of National Natural Science Foundation of China (NSFC 81973169, 21572011, 81573410, 31370741, and 81473106) and the Ministry of Science and Technology of the People's Republic of China (2013CB531302).

ABBREVIATIONS

nAChR, neuronal $\alpha 7$ nicotinic acetylcholine receptor; PAM, positive allosteric modulators; EC_{50} , median effect concentration; $T_{1/2}$, half-life of drug; 5-HT, 5-hydroxytryptamine; hERG, human ether-a-go-go-related gene; ACh, nicotinic acetylcholine; NMDA, N-methyl-D-aspartic acid; GABA, γ aminobutyric acid; PPI, prepulse inhibition; SAR, structure-activity relationship; THF, tetrahydrofuran; CuTC, copper(I) thiophene-2-carboxylate; $Pd(PPh_3)_2Cl_2$, ditriphenylphosphine palladium dichloride; NH_4Cl , ammonium chloride; Ph, phenyl group; CNS, central nervous system; SI, Supporting Information; PK/PD, pharmacokinetics/pharmacodynamics; NADPH, nicotinamide adenine dinucleotide phosphate; BBB, blood-brain barrier; CHO, Chinese hamster ovary; MLA, methyllycaconitine; NMR, nuclear magnetic resonance; $CDCl_3$, deuterated chloroform; DMSO, dimethyl sulfoxide; LC-MS, liquid chromatography-mass spectrometry; Et_3N , triethyl ammonia; PE, petroleum ether; CuTC, copper(I) thiophene-2-carboxylate; EA, ethyl acetate; mp, melting point; HRMS, high-resolution mass spectrometry; HPLC, high-performance liquid chromatography; $Pd(Ph_3P)_4$, tetrakis(triphenylphosphine)palladium(0); TEVC, two-electrode voltage clamp; HEPES, 4-(2-hydroxyethyl)-1-piperazineethanesulfonic acid; cRNA, complementary ribonucleic acid; HEK, human embryonic kidney; CO_2 , carbon dioxide; PEG, poly(ethylene glycol); H_2O , water; ESI, electrospray ionization; IC_{50} , median inhibition concentration; ANOVA, analysis of variance; CuI, copper(I) iodide; dppp, [1,3-bis-(diphenylphosphino)propane]nickel(II) chloride; PSA, polar surface area; Cl_{int} , intrinsic clearance; E_{max} , maximum effect

REFERENCES

- (1) Dani, J. A.; Bertrand, D. Nicotinic acetylcholine receptors and nicotinic cholinergic mechanisms of the central nervous system. *Annu. Rev. Pharmacol. Toxicol.* **2007**, *47*, 699–729.
- (2) Yang, T.; Xiao, T.; Sun, Q.; Wang, K. W. The current agonists and positive allosteric modulators of $\alpha 7$ nAChR for CNS indications in clinical trials. *Acta Pharm. Sin. B* **2017**, *7*, 611–622.
- (3) Freedman, R. $\alpha 7$ -nicotinic acetylcholine receptor agonists for cognitive enhancement in schizophrenia. *Annu. Rev. Med.* **2014**, *65*, 245–261.
- (4) (a) Martin, L. F.; Kem, W. R.; Freedman, R. $\alpha 7$ nicotinic receptor agonists: potential new candidates for the treatment of schizophrenia. *Psychopharmacology* **2004**, *174*, 54–64. (b) Martin, L. F.; Freedman, R. Schizophrenia and the $\alpha 7$ nicotinic acetylcholine receptor. *Int. Rev. Neurobiol.* **2007**, *78*, 225–246.
- (5) (a) Corradi, J.; Bouzat, C. Understanding the bases of function and modulation of $\alpha 7$ nicotinic receptors: Implications for drug discovery. *Mol. Pharmacol.* **2016**, *90*, 288–299. (b) Grønlien, J. H.; Håkerud, M.; Ween, H.; Thorin-Hagene, K.; Briggs, C. A.; Gopalakrishnan, M.; Malysz, J. Distinct profiles of $\alpha 7$ nAChR positive

allosteric modulation revealed by structurally diverse chemotypes. *Mol. Pharmacol.* **2007**, *72*, 715–724.

(6) (a) Hurst, R. S.; Hajos, M.; Raggenbass, M.; Wall, T. M.; Higdon, N. R.; Lawson, J. A.; Rutherford-Root, K. L.; Berkenpas, M. B.; Hoffmann, W. E.; Piotrowski, D. W.; Groppi, V. E.; Allaman, G.; Ogier, R.; Bertrand, S.; Bertrand, D.; Arneric, S. P. A novel positive allosteric modulator of the $\alpha 7$ neuronal nicotinic acetylcholine receptor: in vitro and in vivo characterization. *J. Neurosci.* **2005**, *25*, 4396–4405. (b) Alzarea, S.; Rahman, S. $\alpha 7$ -nicotinic receptor allosteric modulator PNU120596 prevents lipopolysaccharide-induced anxiety, cognitive deficit and depression-like behaviors in mice. *Behav. Brain Res.* **2019**, *366*, 19–28.

(7) Verma, M. K.; Goel, R. N.; Bokare, A. M.; Dandekar, M. P.; Koul, S.; Desai, S.; Tota, S.; Singh, N.; Nigade, P. B.; Patil, V. B.; Modi, D.; Mehta, M.; Gundu, J.; Walunj, S. S.; Karche, N. P.; Sinha, N.; Kamboj, R. K.; Palle, V. P. LL-00066471, a novel positive allosteric modulator of $\alpha 7$ nicotinic acetylcholine receptor ameliorates cognitive and sensorimotor gating deficits in animal models: Discovery and preclinical characterization. *Eur. J. Pharmacol.* **2021**, *891*, No. 173685.

(8) Gill, J. K.; Dhankher, P.; Sheppard, T. D.; Sher, E.; Millar, N. S. A series of $\alpha 7$ nicotinic acetylcholine receptor allosteric modulators with close chemical similarity but diverse pharmacological properties. *Mol. Pharmacol.* **2012**, *81*, 710–718.

(9) Sinha, N.; Karche, N. P.; Verma, M. K.; Walunj, S. S.; Nigade, P. B.; Jana, G.; Kurhade, S. P.; Hajare, A. K.; Tilekar, A. R.; Jadhav, G. R.; Thube, B. R.; Shaikh, J. S.; Balgude, S.; Singh, L. B.; Mahimane, V.; Adurkar, S. K.; Hatnapure, G.; Rajee, F.; Bhosale, Y.; Bhanage, D.; Sachchidanand, S.; Dixit, R.; Gupta, R.; Bokare, A. M.; Dandekar, M.; Bharné, A.; Chatterjee, M.; Desai, S.; Koul, S.; Modi, D.; Mehta, M.; Patil, V.; Singh, M.; Gundu, J.; Goel, R. N.; Shah, C.; Sharma, S.; Bakhle, D.; Kamboj, R. K.; Palle, V. P. Discovery of novel, potent, brain-permeable, and orally efficacious positive allosteric modulator of $\alpha 7$ nicotinic acetylcholine receptor [4-(5-(4-chlorophenyl)-4-methyl-2-propionylthiophen-3-yl)benzenesulfonamide]: structure-activity relationship and preclinical characterization. *J. Med. Chem.* **2020**, *63*, 944–960.

(10) Guerra-Álvarez, M.; Moreno-Ortega, A. J.; Navarro, E.; Fernández-Morales, J. C.; Egea, J.; Lopóez, M. G.; Cano-Abad, M. F. Positive allosteric modulation of $\alpha 7$ nicotinic receptors promotes cell death by inducing Ca^{2+} release from the endoplasmic reticulum. *J. Neurochem.* **2015**, *133*, 309–319.

(11) Harvey, A. J.; Avery, T. D.; Schaeffer, L.; Joseph, C.; Huff, B. C.; Singh, R.; Morice, C.; Giethlen, B.; Grishin, A. A.; Coles, C. J.; Kolesik, P.; Wagner, S.; Andriambeloson, E.; Huyard, B.; Poiraud, E.; Paul, D.; O'Connor, S. M. Discovery of BNC375, a potent, selective, and orally available type I positive allosteric modulator of $\alpha 7$ nAChR. *ACS Med. Chem. Lett.* **2019**, *10*, 754–760.

(12) Timmermann, D. B.; Grønlien, J. H.; Kohlhaas, K. L.; Nielsen, E. O.; Dam, E.; Jorgensen, T. D.; Ahring, P. K.; Peters, D.; Holst, D.; Christensen, J. K.; et al. An allosteric modulator of the $\alpha 7$ nicotinic acetylcholine receptor possessing cognition enhancing properties *in vivo*. *J. Pharmacol. Exp. Ther.* **2007**, *323*, 294–307.

(13) (a) Ng, H. J.; Whittemore, E. R.; Tran, M. B.; Hogenkamp, D. J.; Broide, R. S.; Johnstone, T. B.; Zheng, L.; Stevens, K. E.; Gee, K. W. Nootropic $\alpha 7$ nicotinic receptor allosteric modulator derived from GABA_A receptor modulators. *Proc. Natl. Acad. Sci. U.S.A.* **2007**, *104*, 8059–8064. (b) Nikiforuk, A.; Kos, T.; Potasiewicz, A.; Popik, P. Positive allosteric modulation of $\alpha 7$ nicotinic acetylcholine receptors enhance recognition memory and cognitive flexibility in rats. *Eur. Neuropsychopharmacol.* **2015**, *25*, 1300–1313. (c) Nikiforuk, A.; Kos, T.; Holuj, M.; Potasiewicz, A.; Popik, P. Positive allosteric modulators of $\alpha 7$ nicotinic acetylcholine receptors reverse ketamine-induced schizophrenia-like deficits in rats. *Neuropharmacology* **2016**, *101*, 389–400. (d) Kantrowitz, J. T.; Javitt, D. C.; Freedman, R.; Sehatpour, P.; Kegeles, L. S.; Carlson, M.; Sobeih, T.; Wall, M. M.; Choo, T.-H.; Vail, B.; Grinband, J.; Lieberman, J. A. Double blind, two dose, randomized, placebo-controlled, cross-over clinical trial of the positive allosteric modulator at the $\alpha 7$ nicotinic

cholinergic receptor AVL-3288 in schizophrenia patients. *Neuropsychopharmacology* **2020**, *45*, 1339–1345.

(14) Arias, H. R.; Ghelardini, C.; Lucarini, E.; Tae, H.-S.; Yousuf, A.; Marcovich, I.; Manetti, D.; Romanelli, M. N.; Elgoyhen, A. B.; Adams, D. J.; Mannelli, L. D. C. (E)-3-Furan-2-yl-N-p-tolyl-acrylamide and its derivative DM489 decrease neuropathic pain in mice predominantly by $\alpha 7$ nicotinic acetylcholine receptor potentiation. *ACS Chem. Neurosci.* **2020**, *11*, 3603–3614.

(15) Dinklo, T.; Shaban, H.; Thuring, J. W.; Lavreysen, H.; Stevens, K. E.; Zheng, L.; Mackie, C.; Grantham, C.; Vandenberg, I.; Meulders, G.; Peeters, L.; Verachtert, H.; De Prins, E.; Lesage, A. S. Characterization of 2-[[4-fluoro-3-(trifluoromethyl)phenyl]amino]-4-(4-pyridinyl)-5-thiazolemethanol (JNJ-1930942), a novel positive allosteric modulator of the $\alpha 7$ nicotinic acetylcholine receptor. *J. Pharmacol. Exp. Ther.* **2011**, *336*, S60–S74.

(16) de Vega, M. J. P.; Fernandez-Mendivil, C.; de la Torre Martinez, R.; González-Rodríguez, S.; Mullet, J.; Sala, F.; Sala, S.; Criado, M.; Moreno-Fernández, S.; Miguel, M.; Fernández-Carvajal, A.; Ferrer-Montiel, A.; López, M. G.; González-Muñoz, R. 1-(2',S'-Dihydroxyphenyl)-3-(2-fluoro-4-hydroxyphenyl)-1-propanone (RGM079): A positive allosteric modulator of $\alpha 7$ nicotinic receptors with analgesic and neuroprotective activity. *ACS Chem. Neurosci.* **2019**, *10*, 3900–3909.

(17) Post-Munson, D. J.; Pieschl, R. L.; Molski, T. F.; Graef, J. D.; Hendricson, A. W.; Knox, R. J.; McDonald, I. M.; Olson, R. E.; Macor, J. E.; Weed, M. R.; Bristow, L. J.; Kiss, L.; Ahljianian, M. K.; Herrington, J. B-973, a novel piperazine positive allosteric modulator of the $\alpha 7$ nicotinic acetylcholine receptor. *Eur. J. Pharmacol.* **2017**, *799*, 16–25.

(18) Antonio-Tolentino, K.; Hopkins, C. R. Selective $\alpha 7$ nicotinic receptor agonists and positive allosteric modulators for the treatment of schizophrenia – a review. *Expert Opin. Invest. Drugs* **2020**, *29*, 603–610.

(19) Li, Y. H.; Sun, L. L.; Yang, T. Y.; Jiao, W. X.; Tang, J. S.; Huang, X. M.; Huang, Z. Z.; Meng, Y.; Luo, L. C.; Wang, X. T.; Bian, X. L.; Zhang, F.; Wang, K. W.; Sun, Q. The design and synthesis of novel positive allosteric modulators of $\alpha 7$ nicotinic acetylcholine receptors with the ability to rescue auditory gating deficit in mice. *J. Med. Chem.* **2019**, *62*, 159–173.

(20) (a) Sarhan, M. O.; Motaleb, M. A.; Ibrahim, I. T.; Anwar, M. M.; Zagahy, W. A. Development, potential anticancer activity and the receptor profile of different functionalized 1,3,5-triazine derivatives. *Mini-Rev. Med. Chem.* **2018**, *18*, 1302–1320. (b) Cascioferro, S.; Parrino, B.; Spano, V.; Carbone, A.; Montalbano, A.; Barraja, P.; Diana, P.; Cirrincione, G. 1,3,5-Triazines: A promising scaffold for anticancer drugs development. *Eur. J. Med. Chem.* **2017**, *142*, S23–S49. (c) Iikubo, K.; Kondoh, Y.; Shimada, I.; Matsuya, T.; Mori, K.; Ueno, Y.; Okada, M. Discovery of N-[2-Methoxy-4-[4-(4-methylpiperazin-1-yl)piperidin-1-yl]phenyl]-N'-[2-(propane-2-sulfonyl)-phenyl]-1,3,5-triazine-2,4-diamine (ASP3026), a potent and selective anaplastic lymphoma kinase (ALK) inhibitor. *Chem. Pharm. Bull.* **2018**, *66*, 251–262.

(21) Mibu, N.; Ohata, T.; Sano, M.; Zhou, J.-R.; Yokomizo, K.; Aki, H.; Sumoto, K. Carbohydrate recognition of C3-symmetrical tripodal receptor-type 2,4,6-trisubstituted 1,3,5-triazine derivatives with antiviral activities. *J. Therm. Anal. Calorim.* **2019**, *135*, 2807–2811.

(22) Singh, P.; Kaur, S.; Kumari, P.; Kaur, B.; Kaur, M.; Singh, G.; Bhatti, R.; Bhatti, M. Tailoring the substitution pattern on 1,3,5-triazine for targeting cyclooxygenase-2: Discovery and structure-activity relationship of triazine-4-aminophenylmorpholin-3-one hybrids that reverse algia and inflammation in Swiss albino mice. *J. Med. Chem.* **2018**, *61*, 7929–7941.

(23) (a) Baréa, P.; Barbosa, V. A.; Bidoia, D. L.; Carreira de Paula, J.; Stefanello, T. F.; Ferreira da Costa, W.; Nakamura, C. V.; Sarragiotto, M. H. Synthesis, antileishmanial activity and mechanism of action studies of novel β -carboline-1,3,5-triazine hybrids. *Eur. J. Med. Chem.* **2018**, *150*, 579–590. (b) Salado, I. G.; Baán, A.; Verdeyen, T.; Matheussen, A.; Caljon, G.; Van der Veken, P.; Kiekens, F.; Maes, L.; Augustyns, K. Optimization of the pharmacokinetic properties of

potent antitrypanosomal triazine derivatives. *Eur. J. Med. Chem.* **2018**, *151*, 18–26.

(24) Brown, D.; Cacciola, J.; Jacobs, R. T.; McLaren, F. M.; Shenvi, A. B.; Smith, R. W. J. Preparation of Novel 2,4,6-Trisubstituted Heterocycle Amino Acid Derivatives for Treatment of Neurological Disorders. WO2005003103A2, 2005.

(25) (a) Lee, S.; Phuan, P.-W.; Felix, C. M.; Tan, J.-A.; Levin, M. H.; Verkman, A. S. Nanomolar-potency aminophenyl-1,3,5-triazine activators of the cystic fibrosis transmembrane conductance regulator (CFTR) chloride channel for prosecretory therapy of dry eye diseases. *J. Med. Chem.* **2017**, *60*, 1210–1218. (b) Buchanan, J. L.; Bregman, H.; Chakka, N.; Dimauro, E. F.; Du, B.; Nguyen, H. N.; Zheng, X. M. Preparation of Triazine Compounds as Inhibitors of Voltage-Gated Sodium Channels for Treating Chronic Pain Disorders. WO2010022055A2, 2010.

(26) Tang, J.; Xie, B.; Bian, X.; Xue, Y.; Wei, N.; Zhou, J.; Hao, Y.; Li, G.; Zhang, L.; Wang, K. Identification and *in vitro* pharmacological characterization of a novel and selective $\alpha 7$ nicotinic acetylcholine receptor agonist, Br-IQ17B. *Acta Pharmacol. Sin.* **2015**, *36*, 800–812.

(27) Wager, T. T.; Chandrasekaran, R. Y.; Hou, X.; Troutman, M. D.; Verhoest, P. R.; Villalobos, A.; Will, Y. Defining desirable central nervous system drug space through the alignment of molecular properties, *in vitro* ADME, and safety attributes. *ACS Chem. Neurosci.* **2010**, *1*, 420–434.

(28) Young, G. T.; Zwart, R.; Walker, A. S.; Sher, E.; Millar, N. S. Potentiation of $\alpha 7$ nicotinic acetylcholine receptors via an allosteric transmembrane site. *Proc. Natl. Acad. Sci. U.S.A.* **2008**, *105*, 14686–14691.

(29) Newcombe, J.; Chatzidaki, A.; Sheppard, T. D.; Topf, M.; Millar, N. S. Diversity of nicotinic acetylcholine receptor positive allosteric modulators revealed by mutagenesis and a revised structural model. *Mol. Pharmacol.* **2018**, *93*, 128–140.

(30) Beattie, D. T.; Higgins, D. L.; Ero, M. P.; Amagasa, S. M.; Vickery, R. G.; Kersey, K.; Hopkins, A.; Smith, J. A. M. An *in vitro* investigation of the cardiovascular effects of the 5-HT₄ receptor selective agonists, velusetrag and TD-8954. *Vasc. Pharmacol.* **2013**, *58*, 150–156.

(31) Wang, Y.; Mi, J.; Lu, K.; Lu, Y.; Wang, K. W. Comparison of gating properties and use dependent block of Nav1.5 and Nav1.7 Channels by antiarrhythmics mexiletine and Lidocaine. *PLoS One* **2015**, *10*, No. e0128653.

(32) Baell, J. B.; Holloway, G. A. New substructure filters for removal of pan assay interference compounds (PAINS) from screening libraries and for their exclusion in bioassays. *J. Med. Chem.* **2010**, *53*, 2719–2740.

(33) http://Cbligand.org/PAINS/Search_struct.php.

(34) Junaid, A.; Lim, F. P. L.; Tiekink, E. R. T.; Dolzhenko, A. V. New one-pot synthesis of 1,3,5-triazines: three-component condensation, Dimroth rearrangement and dehydrogenative and dehydrogenative aromatization. *ACS Comb. Sci.* **2019**, *21*, S48–S55.

(35) Niyaz, N. M.; Guenther-Sperger, K. A.; Hunter, R.; Brown, A. V.; Nugent, J. S. Preparation of Insecticidal (1,3,5)-Triazinyl Phenyl Hydrazones. US20090093481A1, 2009.

(36) Zeng, T.; Ren, W. Z. 4,6-Dichloro-N-(4-methoxyphenyl)-1,3,5-triazin-2-amine. *Acta Crystallogr., Sect. E: Struct. Rep. Online* **2007**, *63*, O4622.

(37) Ju, X. L.; Huang, X.; Li, S. T. Preparation of 2-Dimethylamino-4-(4-chloroanilino)-6-(4-trifluoromethyl anilino)-1,3,5-triazine for Insecticide. CN102442960A, 2012.

(38) Kumar, A.; Srivastava, K.; Raja Kumar, S.; Siddiqi, M. I.; Puri, S. K.; Sexana, J. K.; Chauhan, P. M. S. 4-Anilinoquinoline triazines: a novel class of hybrid antimalarial agents. *Eur. J. Med. Chem.* **2011**, *46*, 676–690.